

# Semi-Supervised Clustering via Dynamic Graph Structure Learning

Huaming Ling, Chenglong Bao, *Member, IEEE*, Xin Liang, and Zuoqiang Shi

**Abstract**—Most existing semi-supervised graph-based clustering methods exploit the supervisory information by either refining the affinity matrix or directly constraining the low-dimensional representations of data points. The affinity matrix represents the graph structure and is vital to the performance of semi-supervised graph-based clustering. However, existing methods adopt a static affinity matrix to learn the low-dimensional representations of data points and do not optimize the affinity matrix during the learning process. In this paper, we propose a novel dynamic graph structure learning method for semi-supervised clustering. In this method, we simultaneously optimize the affinity matrix and the low-dimensional representations of data points by leveraging the given pairwise constraints. Moreover, we propose an alternating minimization approach with proven convergence to solve the proposed nonconvex model. During the iteration process, our method cyclically updates the low-dimensional representations of data points and refines the affinity matrix, leading to a dynamic affinity matrix (graph structure). Specifically, for the update of the affinity matrix, we enforce the data points with remarkably different low-dimensional representations to have an affinity value of 0. Furthermore, we construct the initial affinity matrix by integrating the local distance and global self-representation among data points. Experimental results on eight benchmark datasets under different settings show the advantages of the proposed approach.

**Index Terms**—Semi-supervised clustering, graph-based clustering, low-dimensional representations, nonconvex optimization, dynamic graph structure.

## I. INTRODUCTION

CLUSTERING is an important problem in data mining and machine learning. Clustering aims to partition a set of data points into several groups so that data points in the same group (cluster) are more similar to each other than those in other groups (clusters). Besides the data points, clustering methods do not require any supervisory information. In practice, although it is difficult to obtain the exact label information, partial/weak supervisory information is available. One common supervisory information is given in the form of pairwise constraints, including must-link (ML) constraints (the pair of data points must belong to the same cluster) and cannot-link (CL) constraints (the pair of data points must belong to different clusters). Thus, semi-supervised clustering is to cluster data points by exploring the supervisory information and has been extensively studied during the past two decades, such as [1]–[8]. Moreover, semi-supervised clustering has been

widely applied in many tasks including medical diagnosis [9], natural language processing [10], bioinformatics [11], image processing [12], [13], social networks [14] and information networks [15].

Among clustering methods, one important branch is graph-based clustering like spectral clustering (SC) [16]. The performance of graph-based methods highly depends on the quality of the graph structure (affinity matrix) that represents the similarity among data points. Most of the existing semi-supervised graph-based clustering methods explore the supervisory information in the following two ways [17]: 1) refining the affinity matrix with the supervisory information; 2) constraining the low-dimensional representations with the supervisory information. For the first way, [18] sets the corresponding element of the affinity matrix to 1 (resp. 0) if the two data points belong to ML (resp. CL). In [19], a positive (resp. negative) term is added to the corresponding element of the affinity matrix if the two data points belong to ML (resp. CL). Furthermore, [20] refines the affinity matrix through an affinity propagation method. [21] introduces a novel cannot-link graph regularization to enforce cannot-link constrained data points in different clusters. For the second way, [22] proposes a constrained spectral clustering model to adapt the spectral representation towards an ideal representation as consistent with the pairwise constraints as possible. [23] and [24] propose a constrained spectral clustering model which uses a user-specific parameter to constrain how well the pairwise constraints are satisfied. [14] introduces a semi-supervised clustering model to enforce the low-dimensional representations of ML constrained data points to be similar.

The performance of semi-supervised graph-based clustering highly depends on the affinity matrix. However, these methods do not change the affinity matrix during the learning of low-dimensional representations of data points, leading to a static affinity matrix. In this paper, we introduce a dynamic graph structure learning method for semi-supervised clustering. Given the initial affinity matrix, we propose a unified optimization framework to simultaneously optimize the affinity matrix itself and the low-dimensional representations of data points with the guidance of the given pairwise constraints, as shown in Fig. 1. In the unified optimization framework, we cyclically update the low-dimensional representations of data points and refine the affinity matrix during the iteration process. Specifically, we enforce the data points that belong to ML (resp. CL) to have similar (resp. different) low-dimensional representations. For the update of the affinity matrix, we enforce the data points with remarkably distinct low-dimensional representations to have an affinity value of

H. Ling, C. Bao, X. Liang and Z. Shi are with the Yau Mathematical Sciences Center, Tsinghua University and Yanqi Lake Beijing Institute of Mathematical Sciences and Applications, Beijing 100084, China (e-mail: linghm18@mails.tsinghua.edu.cn; clbao@mail.tsinghua.edu.cn; liangx-inslm@tsinghua.edu.cn; zqshi@mail.tsinghua.edu.cn).

C. Bao and Z. Shi are the co-corresponding authors.

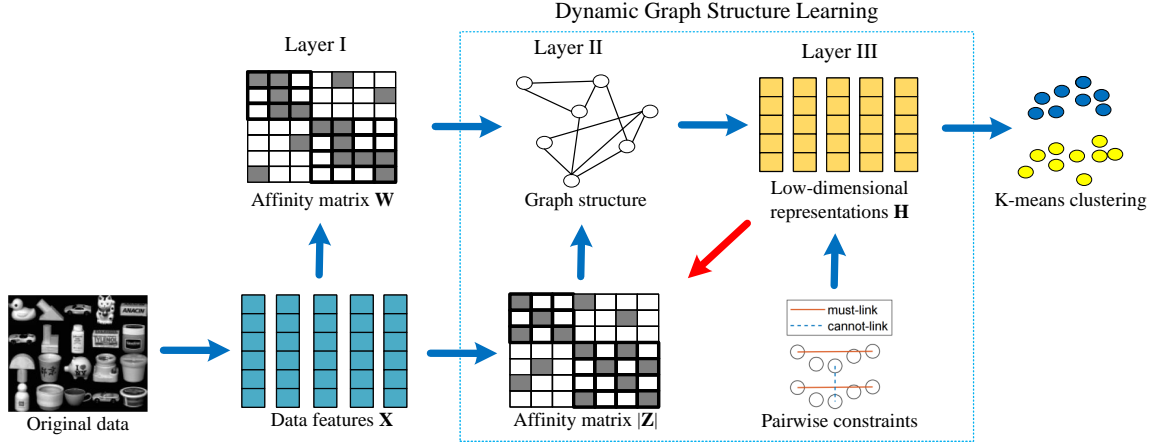


Fig. 1. Illustration of the Dynamic Graph Structure Learning (DGSL) method for semi-supervised clustering. We simultaneously learn the affinity matrix  $|Z|$  and the low-dimensional representations  $H$  for all data points with the guidance of the given pairwise constraints. We construct the graph structure by integrating the local distance ( $W$ ) and global self-representation ( $|Z|$ ) among data points. During the learning process, DGSL cyclically updates the low-dimensional representations  $H$  with the graph structure as well as the pairwise constraints and refines the affinity matrix  $|Z|$  with  $H$ , leading to a dynamic graph structure.

0. Thus the affinity matrix (graph structure) is dynamically updated during the cyclically updating process.

As a comparison, approaches in [25]–[27] integrate the construction of the affinity matrix and the propagation of the partial labels into a unified optimization framework. However, these approaches use partial labels as supervisory information and learn the label matrix for all data points. Our method uses pairwise constraints as supervisory information and learns the low-dimensional representations for all data points. Moreover, the affinity matrix in [25]–[27] is constructed based on the global self-representation model. We obtain the affinity matrix by integrating the local distance and global self-representation among data points. Existing approaches that define affinity can be roughly divided into two categories: 1) the first category connects each data point to its  $m$  nearest neighbors which are defined according to the Euclidean distance, e.g., [28]–[31]; and 2) the second category represents each data point as a linear combination of all data points and induces the affinity by the representation coefficients, e.g., [32]–[34]. Approaches in the first category only connect each data point to its  $m$  nearest neighbors but neglect those “non-neighbor” data points with the same class label, while approaches in the second category connect each data point to other data points in the same linear subspace. We construct the affinity matrix by integrating these two categories, and our main contributions are as follows.

- We propose a novel dynamic graph structure learning method for semi-supervised clustering. Specifically, we introduce a unified optimization framework to simultaneously optimize the graph structure (affinity matrix) and the low-dimensional representations of data points by leveraging pairwise constraints. Moreover, we construct the affinity matrix by integrating the local Euclidean distance and global self-representation among data points.
- We propose an alternating minimization solver to solve the proposed nonconvex model with proven convergence. Specifically, the graph structure and the low-dimensional representations of data points are cyclically updated in

the alternating minimization solver. Moreover, at each iteration, we refine the graph structure based on the low-dimensional representations of data points, leading to a dynamic graph structure.

- We evaluate our approach in eight benchmark datasets and compare it with several state-of-the-art semi-supervised graph-based clustering methods. Extensive experiments have been conducted under different settings of pairwise constraints to show the effectiveness of our approach. Moreover, we extend our approach to hypergraph datasets and achieve competitive performance compared with state-of-the-art hypergraph learning methods.

## II. RELATED WORK

**Notations.** We denote matrices by boldface uppercase letters, e.g.,  $W$ , vectors by boldface lowercase letters, e.g.,  $h$ , and scalars by lowercase letters, e.g.,  $w$ . We denote  $w_{ij}$  or  $W_{ij}$  as the  $(i, j)$ -th element of  $W$  and denote  $w_i$  as the  $i$ -th column of  $W$ . We use  $\text{Tr}(W)$  to denote the trace of  $W$ .  $|W|$  is the matrix consisting of the absolute value of each element of  $W$ . We denote  $\text{diag}(W)$  as a diagonal matrix with its  $i$ -th diagonal element being the  $i$ -th diagonal element of  $W$  and denote  $W^T$  as the transpose of  $W$ . We set  $I$  as the identity matrix and  $0$  as a matrix of all zeros. We give the notations of some norms, e.g.,  $\ell_1$ -norm  $\|W\|_1 = \sum_{ij} |w_{ij}|$ ,  $\ell_\infty$ -norm  $\|w\|_\infty = \max_i |w_i|$  and Frobenius norm (or  $\ell_2$ -norm of a vector)  $\|W\| = \sqrt{\sum_{ij} w_{ij}^2}$ .

### A. Subspace Clustering

Many high-dimensional datasets approximately lie on the union of multiple low-dimensional linear subspaces. For example, we can model the motion trajectories in a video, face images, and hand-written digits as the union of subspaces, with each subspace corresponding to a class. Such a subspace structure has motivated the problem of subspace clustering, which aims to group the data points into clusters, with each

cluster corresponding to a subspace. Subspace clustering has been applied in many areas, such as motion segmentation [35], face clustering [36], and image processing [37]. Subspace clustering represents each data point as a linear combination of other data points. Such a representation is not unique, and sparse subspace clustering (SSC) [35] pursues a sparse representation by solving the following problem

$$\min_{\mathbf{Z}} \|\mathbf{Z}\|_1 + \gamma \|\mathbf{X} - \mathbf{XZ}\|_1, \text{ s.t. } \text{diag}(\mathbf{Z}) = \mathbf{0}, \quad (1)$$

where  $\mathbf{Z} = (z_{ij}) \in \mathbb{R}^{n \times n}$  is the self-representation matrix for  $n$  data points  $\mathbf{X} = [\mathbf{x}_1, \mathbf{x}_2, \dots, \mathbf{x}_n]$ , and  $|z_{ij}|$  reflects the affinity between data point  $\mathbf{x}_i$  and data point  $\mathbf{x}_j$ .  $\|\mathbf{X} - \mathbf{XZ}\|_1$  measures the representation error and outliers. Then the affinity matrix is obtained by  $\frac{1}{2}(|\mathbf{Z}| + |\mathbf{Z}|^\top)$ , which is further used for SC [16] to obtain the final clustering results.

### B. Spectral Clustering

Spectral Clustering (SC) [16] is one of the most important clustering methods. Given an affinity matrix  $\mathbf{W} \in \mathbb{R}^{n \times n}$  of  $n$  data points  $\mathbf{X} = [\mathbf{x}_1, \mathbf{x}_2, \dots, \mathbf{x}_n] \in \mathbb{R}^{d \times n}$ , SC first obtains the low-dimensional representations  $\mathbf{H} = [\mathbf{h}_1, \mathbf{h}_2, \dots, \mathbf{h}_n] \in \mathbb{R}^{k \times n}$  for all data points by solving

$$\min_{\mathbf{H}} \text{Tr}(\mathbf{H}\mathbf{L}\mathbf{H}^\top), \text{ s.t. } \mathbf{H}\mathbf{H}^\top = \mathbf{I}, \quad (2)$$

where  $\mathbf{L} = \mathbf{I} - \mathbf{D}^{-1/2}\mathbf{W}\mathbf{D}^{-1/2}$  is the normalized Laplacian matrix and  $\mathbf{D}$  is the diagonal matrix with each diagonal element  $d_{ii} = \sum_{j=1}^n w_{ij}$ . The optimal solution of (2) can be obtained by computing the  $k$  eigenvectors of  $\mathbf{L}$  corresponding to the  $k$  smallest eigenvalues. Then SC computes  $\hat{\mathbf{H}} \in \mathbb{R}^{k \times n}$  by normalizing each column of  $\mathbf{H}$  into unit Euclidean length and performs K-means on the columns of  $\hat{\mathbf{H}}$  to obtain the final clustering results.

### C. Linear Discriminant Analysis

The Linear Discriminant Analysis (LDA) [38], [39] is a popular approach in supervised learning for feature extraction and dimensionality reduction. Given a set of  $n$  training data points  $\{\mathbf{x}_i\}_{i=1}^n \in \mathbb{R}^d$  and the corresponding labels  $\{y_i\}_{i=1}^n$ , with  $y_i \in \{1, 2, \dots, c\}$ , LDA finds the linear transformation matrix  $\mathbf{G} \in \mathbb{R}^{m \times d}$  to project high-dimensional vectors,  $\mathbf{x}_1, \mathbf{x}_2, \dots, \mathbf{x}_n \in \mathbb{R}^d$ , into low-dimensional vectors,  $\mathbf{G}\mathbf{x}_1, \mathbf{G}\mathbf{x}_2, \dots, \mathbf{G}\mathbf{x}_n \in \mathbb{R}^m$ , by simultaneously maximizing the inter-class scatter and minimizing the intra-class scatter in the low-dimensional space

$$\mathbf{G}^* = \arg \max_{\mathbf{G}\mathbf{G}^\top = \mathbf{I}} \frac{\sum_{i=1}^c \frac{n_i}{n} \|\mathbf{G}\mathbf{m}_i - \mathbf{G}\mathbf{m}\|^2}{\sum_{i=1}^c \frac{n_{y_i}}{n} \|\mathbf{G}\mathbf{x}_i - \mathbf{G}\mathbf{m}_{y_i}\|^2}, \quad (3)$$

where  $\mathbf{m}_i$  is the centroid of the data points belonging to the  $i$ -th class and  $\mathbf{m}$  is the centroid of all data points, and  $n_i$  is the number of data points belonging to the  $i$ -th class. The problem (3) can be rewritten as a trace ratio problem

$$\mathbf{G}^* = \arg \max_{\mathbf{G}\mathbf{G}^\top = \mathbf{I}} \frac{\text{Tr}(\mathbf{G}\mathbf{S}_b\mathbf{G}^\top)}{\text{Tr}(\mathbf{G}\mathbf{S}_w\mathbf{G}^\top)}, \quad (4)$$

where  $\mathbf{S}_w = \sum_{i=1}^n \frac{n_{y_i}}{n} (\mathbf{x}_i - \mathbf{m}_{y_i})(\mathbf{x}_i - \mathbf{m}_{y_i})^\top$  is the intra-class scatter matrix and  $\mathbf{S}_b = \sum_{i=1}^c \frac{n_i}{n} (\mathbf{m}_i - \mathbf{m})(\mathbf{m}_i - \mathbf{m})^\top$  is the inter-class scatter matrix.

## III. SEMI-SUPERVISED CLUSTERING VIA DYNAMIC GRAPH STRUCTURE LEARNING

### A. Problem Formulation

Given a set of data points  $\mathcal{X} = \{\mathbf{x}_i\}_{i=1}^n$  and the sets of pairwise constraints,  $\mathcal{M}$  and  $\mathcal{C}$ , with

$$\begin{aligned} \mathcal{M} &= \{(\mathbf{x}_i, \mathbf{x}_j) | \mathbf{x}_i \text{ and } \mathbf{x}_j \text{ belong to the same cluster}\}, \\ \mathcal{C} &= \{(\mathbf{x}_i, \mathbf{x}_j) | \mathbf{x}_i \text{ and } \mathbf{x}_j \text{ belong to different clusters}\}, \end{aligned} \quad (5)$$

we aim to learn the low-dimensional representations  $\mathbf{H}$  for all data points such that the intra-class distance is small and the inter-class distance is relatively large for  $\mathbf{H}$ . Then we conduct K-means on  $\mathbf{H}$  to obtain the final clustering results. We formulate the original feature matrix as  $\mathbf{X} = [\mathbf{x}_1, \mathbf{x}_2, \dots, \mathbf{x}_n] \in \mathbb{R}^{d \times n}$  and the low-dimensional representations as  $\mathbf{H} = [\mathbf{h}_1, \mathbf{h}_2, \dots, \mathbf{h}_n] \in \mathbb{R}^{k \times n}$ , with  $\mathbf{h}_i$  corresponding to the low-dimensional representation of  $\mathbf{x}_i$ . In this paper, we set the dimension  $k$  of low-dimensional representation  $\mathbf{h}_i$  as the total number of classes for dataset  $\mathcal{X}$ . For notation convenience, we encode the pairwise constraints into two matrices,  $\mathbf{M} = (m_{ij})$  and  $\mathbf{C} = (c_{ij})$ , with

$$m_{ij} = \begin{cases} 1, & \text{if } (\mathbf{x}_i, \mathbf{x}_j) \in \mathcal{M} \\ 0, & \text{otherwise} \end{cases}, \quad c_{ij} = \begin{cases} \frac{1}{n_c}, & \text{if } (\mathbf{x}_i, \mathbf{x}_j) \in \mathcal{C} \\ 0, & \text{otherwise} \end{cases} \quad (6)$$

where  $n_c$  is the total number of cannot-link constraints in  $\mathcal{C}$ . We use the affinity matrix  $\mathbf{S} = (s_{ij})$  (which will be defined in (10)) and the matrices,  $\mathbf{M}$  and  $\mathbf{C}$ , to learn the low-dimensional representations  $\mathbf{H}$  by solving the constrained optimization problem

$$\arg \min_{\mathbf{H}\mathbf{H}^\top = \mathbf{I}} \frac{\sum_{i,j=1}^n s_{ij} \|\mathbf{h}_i - \mathbf{h}_j\|^2 + \lambda_M \sum_{i,j=1}^n m_{ij} \|\mathbf{h}_i - \mathbf{h}_j\|^2}{\sum_{i,j=1}^n c_{ij} \|\mathbf{h}_i - \mathbf{h}_j\|^2}, \quad (7)$$

where  $\lambda_M > 0$  is a tradeoff parameter and  $s_{ij} \geq 0$  is the affinity value between  $\mathbf{x}_i$  and  $\mathbf{x}_j$ . We enforce the pair of data points with must-link (resp. cannot-link) constraint to have similar (resp. different) low-dimensional representations by minimizing  $\sum_{i,j=1}^n m_{ij} \|\mathbf{h}_i - \mathbf{h}_j\|^2$  and maximizing  $\sum_{i,j=1}^n c_{ij} \|\mathbf{h}_i - \mathbf{h}_j\|^2$  simultaneously in (7). Moreover, to exploit the information of all data points, we also minimize the term  $\sum_{i,j=1}^n s_{ij} \|\mathbf{h}_i - \mathbf{h}_j\|^2$  in (7). The role of minimizing this term is twofold. When the low-dimensional representations  $\mathbf{H}$  is fixed, minimizing this term enforces  $s_{ij}$  equal to 0 whenever  $\|\mathbf{h}_i - \mathbf{h}_j\|^2$  is relatively large. In other words, minimizing this term enforces data points with remarkably different low-dimensional representations to have an affinity value of 0. When the affinity matrix  $\mathbf{S}$  is fixed, minimizing this term enforces  $\mathbf{h}_i = \mathbf{h}_j$  whenever  $s_{ij}$  is relatively large.

The construction of the affinity matrix  $\mathbf{S}$  is essential to the learning of the low-dimensional representations  $\mathbf{H}$ . To fully exploit the pairwise relations among data points, we construct the affinity matrix  $\mathbf{S}$  by integrating the local distance and global self-representation among data points. Specifically, the

affinity matrix  $\mathbf{W} = (w_{ij}) \in \mathbb{R}^{n \times n}$  based on the Euclidean distance is constructed by

$$w_{ij} = \begin{cases} \exp\left(-\frac{\|\mathbf{x}_i - \mathbf{x}_j\|^2}{\sigma_i^2}\right), & \text{if } \mathbf{x}_j \in \mathcal{N}_i \\ 0, & \text{otherwise} \end{cases} \quad (8)$$

where  $\sigma_i$  is defined as the distance from  $\mathbf{x}_i$  to its  $l$ -th nearest neighbor and  $\mathcal{N}_i$  is the set of the  $m$  nearest neighbors of  $\mathbf{x}_i$ . The affinity matrix  $|\mathbf{Z}| \in \mathbb{R}^{n \times n}$  based on the global self-representation model is constructed by solving the problem

$$\min_{\mathbf{Z}} \frac{1}{2} \|\mathbf{X} - \mathbf{XZ}\|^2 + \lambda_Z \|\mathbf{Z}\|_1, \text{ s.t. } \text{diag}(\mathbf{Z}) = \mathbf{0}, \quad (9)$$

where  $\lambda_Z > 0$  is a tradeoff parameter. We apply the Frobenius norm on the reconstruction loss to alleviate the noise effect.  $\ell_1$ -norm is applied to enforce the sparsity of the self-representation matrix  $\mathbf{Z}$ . Then we construct the affinity matrix  $\mathbf{S}$  as the weighted sum of  $\mathbf{W}$  and  $|\mathbf{Z}|$

$$\mathbf{S} = \alpha_1 |\mathbf{Z}| + \alpha_2 \mathbf{W}, \quad (10)$$

where  $\alpha_1 > 0$  and  $\alpha_2 > 0$ .

*Proposition 1:* Given any matrix  $\mathbf{S} \in \mathbb{R}^{n \times n}$ , we define  $\mathbf{L}_\mathbf{S}$  as the Laplacian matrix of  $\frac{|\mathbf{S}| + |\mathbf{S}|^\top}{2}$ , i.e.,  $\mathbf{L}_\mathbf{S} = \mathbf{D}_\mathbf{S} - \frac{|\mathbf{S}| + |\mathbf{S}|^\top}{2}$ , where  $\mathbf{D}_\mathbf{S}$  is a diagonal matrix with the  $i$ -th diagonal element being  $\sum_{j=1}^n \frac{|s_{ij}| + |s_{ji}|}{2}$ . Then we can obtain the following equation

$$\text{Tr}(\mathbf{H} \mathbf{L}_\mathbf{S} \mathbf{H}^\top) = \frac{1}{2} \sum_{i,j=1}^n |s_{ij}| \|\mathbf{h}_i - \mathbf{h}_j\|^2. \quad (11)$$

The proof of Proposition 1 can be found in the Appendix. Then by integrating (7), (9), (10) and Proposition 1, we formulate a unified optimization framework to learn the affinity matrix  $|\mathbf{Z}|$  and the low-dimensional representations  $\mathbf{H}$  simultaneously

$$\begin{aligned} \min_{\mathbf{Z}, \mathbf{H}} \quad & \frac{1}{2} \|\mathbf{X} - \mathbf{XZ}\|^2 + \lambda_Z \|\mathbf{Z}\|_1 + \frac{\alpha_1 \text{Tr}(\mathbf{H} \mathbf{L}_\mathbf{Z} \mathbf{H}^\top)}{\text{Tr}(\mathbf{H} \mathbf{L}_\mathbf{C} \mathbf{H}^\top)} \\ & + \frac{\alpha_2 \text{Tr}(\mathbf{H} (\mathbf{L}_\mathbf{W} + \lambda_M \mathbf{L}_\mathbf{M}) \mathbf{H}^\top)}{\text{Tr}(\mathbf{H} \mathbf{L}_\mathbf{C} \mathbf{H}^\top)}, \quad (12) \\ \text{s.t.} \quad & \text{diag}(\mathbf{Z}) = \mathbf{0}, \mathbf{H} \mathbf{H}^\top = \mathbf{I}, \end{aligned}$$

where  $\lambda_Z > 0$ ,  $\alpha_1 > 0$ ,  $\alpha_2 > 0$  and  $\lambda_M > 0$  are tradeoff parameters. Introducing an auxiliary variable  $\mathbf{A}$ , we consider the penalized problem of (12):

$$\begin{aligned} \min_{\mathbf{A}, \mathbf{Z}, \mathbf{H}} \quad & \frac{1}{2} \|\mathbf{X} - \mathbf{XA}\|^2 + \frac{\lambda}{2} \|\mathbf{A} - \mathbf{Z}\|^2 + \lambda_Z \|\mathbf{Z}\|_1 \\ & + \frac{\alpha_1 \text{Tr}(\mathbf{H} \mathbf{L}_\mathbf{Z} \mathbf{H}^\top)}{\text{Tr}(\mathbf{H} \mathbf{L}_\mathbf{C} \mathbf{H}^\top)} + \frac{\alpha_2 \text{Tr}(\mathbf{H} (\mathbf{L}_\mathbf{W} + \lambda_M \mathbf{L}_\mathbf{M}) \mathbf{H}^\top)}{\text{Tr}(\mathbf{H} \mathbf{L}_\mathbf{C} \mathbf{H}^\top)}, \quad (13) \\ \text{s.t.} \quad & \text{diag}(\mathbf{Z}) = \mathbf{0}, \mathbf{H} \mathbf{H}^\top = \mathbf{I}, \end{aligned}$$

where  $\lambda > 0$  is a parameter with a relatively large value. As will be seen in Section III-B, the term  $\frac{\lambda}{2} \|\mathbf{A} - \mathbf{Z}\|^2$  makes the subproblems for updating  $\mathbf{A}$  and  $\mathbf{Z}$  strongly convex and thus the solutions are unique and stable. This is also beneficial to the convergence analysis.

---

**Algorithm 1** Update  $\mathbf{H}$  by Solving (16) or (24)

---

**Input:**  $\mathbf{B} = \mathbf{L}_\mathbf{C}$ ,  $\mathbf{E} = \mathbf{L}_{\widetilde{\mathbf{W}}}$  for (16) or  $\mathbf{E} = \mathbf{N}_{\widetilde{\mathbf{W}}}$  for (24), dimension  $k$  of low-dimensional representations  $\mathbf{H}$ .

**Initialize:**  $\mathbf{H} \in \mathbb{R}^{k \times n}$ ,  $\mathbf{H} \mathbf{H}^\top = \mathbf{I}$ ,  $\rho := \frac{\text{Tr}(\mathbf{H} \mathbf{B} \mathbf{H}^\top)}{\text{Tr}(\mathbf{H} \mathbf{E} \mathbf{H}^\top)}$ .

**while** not converged **do**

1) Obtain the  $k$  largest eigenvalues of  $\mathbf{B} - \rho \mathbf{E}$  and associated orthonormal eigenvectors  $[\mathbf{v}_1, \mathbf{v}_2, \dots, \mathbf{v}_k]^\top \equiv \mathbf{H}$ ;

2) Set  $\rho := \frac{\text{Tr}(\mathbf{H} \mathbf{B} \mathbf{H}^\top)}{\text{Tr}(\mathbf{H} \mathbf{E} \mathbf{H}^\top)}$ ;

**end while**

**Output:**  $\mathbf{H}$ .

---



---

**Algorithm 2** Solve (13) by Alternating Minimization

---

**Input:** Feature matrix  $\mathbf{X}$ , must-link matrix  $\mathbf{M}$ , cannot-link matrix  $\mathbf{C}$  and matrix  $\mathbf{W}$ , parameters  $\lambda_Z$ ,  $\alpha_1$ ,  $\alpha_2$ ,  $\lambda$  and  $\lambda_M$ .

**Initialize:**  $k = 0$ ,  $\mathbf{A} = \mathbf{0}$ ,  $\mathbf{Z} = \mathbf{0}$ ,  $\mathbf{H} = \mathbf{0}$ .

**while** not converged **do**

1) Compute  $\mathbf{H}^{k+1}$  by solving (16) using Algorithm 1;

2) Compute  $\mathbf{A}^{k+1}$  according to (18);

3) Compute  $\mathbf{Z}^{k+1}$  according to (22);

4)  $k = k + 1$ ;

**end while**

**Output:**  $\mathbf{A} = \mathbf{A}^k$ ,  $\mathbf{Z} = \mathbf{Z}^k$  and  $\mathbf{H} = \mathbf{H}^k$ .

---

### B. Numerical Algorithm

In this section, we show how to solve the nonconvex problem (13). There are three blocks of variables in problem (13) and we adopt the alternating minimization method that cyclically updates  $\{\mathbf{A}\}$ ,  $\{\mathbf{Z}\}$ ,  $\{\mathbf{H}\}$ .

• First, fix  $\mathbf{A} = \mathbf{A}^k$ ,  $\mathbf{Z} = \mathbf{Z}^k$ , and update  $\mathbf{H}^{k+1}$  by

$$\mathbf{H}^{k+1} = \arg \min_{\mathbf{H} \mathbf{H}^\top = \mathbf{I}} \frac{\text{Tr}(\mathbf{H} \mathbf{L}_{\widetilde{\mathbf{W}}} \mathbf{H}^\top)}{\text{Tr}(\mathbf{H} \mathbf{L}_\mathbf{C} \mathbf{H}^\top)}, \quad (14)$$

where

$$\begin{aligned} \widetilde{\mathbf{W}} &= \alpha_1 |\mathbf{Z}| + \alpha_2 (\mathbf{W} + \lambda_M \mathbf{M}), \\ \mathbf{L}_{\widetilde{\mathbf{W}}} &= \alpha_1 \mathbf{L}_\mathbf{Z} + \alpha_2 (\mathbf{L}_\mathbf{W} + \lambda_M \mathbf{L}_\mathbf{M}). \end{aligned} \quad (15)$$

For (14), it is equivalent to

$$\mathbf{H}^{k+1} = \arg \max_{\mathbf{H} \mathbf{H}^\top = \mathbf{I}} \frac{\text{Tr}(\mathbf{H} \mathbf{L}_\mathbf{C} \mathbf{H}^\top)}{\text{Tr}(\mathbf{H} \mathbf{L}_{\widetilde{\mathbf{W}}} \mathbf{H}^\top)}. \quad (16)$$

The trace ratio problem (16) has been efficiently solved by the ALGORITHM 4.1 in [40], which is also shown in Algorithm 1 in this paper.

• Second, fix  $\mathbf{H} = \mathbf{H}^{k+1}$ ,  $\mathbf{Z} = \mathbf{Z}^k$ , and update  $\mathbf{A}^{k+1}$  by

$$\mathbf{A}^{k+1} = \arg \min_{\mathbf{A}} \frac{1}{2} \|\mathbf{X} - \mathbf{XA}\|^2 + \frac{\lambda}{2} \|\mathbf{A} - \mathbf{Z}\|^2. \quad (17)$$

Since the objective function in (17) is smooth and strongly convex, the closed form solution of  $\mathbf{A}^{k+1}$  can be obtained by

$$\mathbf{A}^{k+1} = (\mathbf{X}^\top \mathbf{X} + \lambda \mathbf{I})^{-1} (\mathbf{X}^\top \mathbf{X} + \lambda \mathbf{Z}). \quad (18)$$

• Third, fix  $\mathbf{H} = \mathbf{H}^{k+1}$ ,  $\mathbf{A} = \mathbf{A}^{k+1}$ , and update  $\mathbf{Z}^{k+1}$  by

$$\begin{aligned} \mathbf{Z}^{k+1} &= \arg \min_{\mathbf{Z}} \frac{\alpha_1 \text{Tr}(\mathbf{H} \mathbf{L}_\mathbf{Z} \mathbf{H}^\top)}{\text{Tr}(\mathbf{H} \mathbf{L}_\mathbf{C} \mathbf{H}^\top)} + \frac{\lambda}{2} \|\mathbf{Z} - \mathbf{A}\|^2 + \lambda_Z \|\mathbf{Z}\|_1, \\ \text{s.t.} \quad & \text{diag}(\mathbf{Z}) = \mathbf{0}. \end{aligned} \quad (19)$$

**Algorithm 3** Solve (13) by Alternating Minimization and Normalization Operations

**Input:** Feature matrix  $\mathbf{X}$ , must-link matrix  $\mathbf{M}$ , cannot-link matrix  $\mathbf{C}$  and matrix  $\mathbf{W}$ , parameters  $\lambda_Z$ ,  $\alpha_1$ ,  $\alpha_2$ ,  $\lambda$  and  $\lambda_M$ .

**Initialize:**  $k = 0$ ,  $\mathbf{A} = \mathbf{0}$ ,  $\mathbf{Z} = \mathbf{0}$ ,  $\mathbf{H} = \mathbf{0}$ .

**while** not converged **do**

- 1) Obtain  $\tilde{\mathbf{W}}$  by (23);
- 2) Compute  $\mathbf{H}^{k+1}$  by solving (24) using Algorithm 1;
- 3) Compute  $\mathbf{A}^{k+1}$  according to (18);
- 4) Obtain  $\Theta$  by (25);
- 5) Compute  $\mathbf{Z}^{k+1}$  according to (22);
- 6)  $k=k+1$ ;

**end while**

**Output:**  $\mathbf{A} = \mathbf{A}^k$ ,  $\mathbf{Z} = \mathbf{Z}^k$  and  $\mathbf{H} = \mathbf{H}^k$ .

Since  $\text{Tr}(\mathbf{H}\mathbf{L}_Z\mathbf{H}^\top) = \frac{1}{2} \sum_{i,j=1}^n |z_{ij}| \|\mathbf{h}_i - \mathbf{h}_j\|^2$  from Proposition 1 and  $\|\mathbf{Z}\|_1 := \sum_{i,j=1}^n |z_{ij}|$ , we can rewrite (19) as

$$\mathbf{Z}^{k+1} = \arg \min_{\mathbf{Z}} \frac{1}{2} \|\mathbf{Z} - \mathbf{A}\|^2 + \|\Theta \odot \mathbf{Z}\|_1, \text{ s.t. } \text{diag}(\mathbf{Z}) = \mathbf{0}, \quad (20)$$

where  $\odot$  is the Hadamard product and  $\Theta = (\Theta_{ij})$ , with

$$\Theta_{ij} = \frac{\alpha_1 \|\mathbf{h}_i - \mathbf{h}_j\|^2}{2\lambda \text{Tr}(\mathbf{H}\mathbf{L}_C\mathbf{H}^\top)} + \frac{\lambda_Z}{\lambda}. \quad (21)$$

The closed form solution for (20) can be calculated by

$$\mathbf{Z}^{k+1} = \hat{\mathbf{Z}}^{k+1} - \text{diag}(\hat{\mathbf{Z}}^{k+1}), \quad (22)$$

where  $\hat{\mathbf{Z}}_{ij}^{k+1} = \text{sgn}(\mathbf{A}_{ij}) \max(|\mathbf{A}_{ij}| - \Theta_{ij}, 0)$  and  $\text{sgn}(a) := 1$  (resp.  $0$ ,  $-1$ ) if  $a > 0$  (resp.  $a = 0$ ,  $a < 0$ ). The whole procedure of the alternating minimization scheme for (13) is given in Algorithm 2.

Furthermore, to boost the performance of our model, we adopt normalization operations during the updating procedure for  $\mathbf{A}, \mathbf{Z}, \mathbf{H}$ . Specifically, for the update of  $\mathbf{H}^{k+1}$ , we first construct the matrix  $\tilde{\mathbf{W}}$  as

$$\tilde{\mathbf{w}}_i = \alpha_1 \frac{|\mathbf{z}_i|}{\|\mathbf{z}_i\|_\infty} + \alpha_2 (\mathbf{w}_i + \lambda_M \mathbf{m}_i), \quad i = 1, \dots, n, \quad (23)$$

where  $\tilde{\mathbf{w}}_i$  is the  $i$ -th column of  $\tilde{\mathbf{W}}$ . Then we obtain  $\mathbf{H}^{k+1}$  by solving the optimization problem

$$\mathbf{H}^{k+1} = \arg \max_{\mathbf{H} \mathbf{H}^\top = \mathbf{I}} \frac{\text{Tr}(\mathbf{H}\mathbf{L}_C\mathbf{H}^\top)}{\text{Tr}(\mathbf{H}\mathbf{N}_{\tilde{\mathbf{W}}}\mathbf{H}^\top)}, \quad (24)$$

where  $\mathbf{N}_{\tilde{\mathbf{W}}}$  is the normalization of the Laplacian matrix  $\mathbf{L}_{\tilde{\mathbf{W}}}$ , i.e.,  $\mathbf{N}_{\tilde{\mathbf{W}}} = \mathbf{D}_{\tilde{\mathbf{W}}}^{-1/2} \mathbf{L}_{\tilde{\mathbf{W}}} \mathbf{D}_{\tilde{\mathbf{W}}}^{-1/2}$ , and  $\mathbf{D}_{\tilde{\mathbf{W}}}$  is a diagonal matrix with its  $i$ -th diagonal element being  $\sum_{j=1}^n \frac{\tilde{\mathbf{w}}_{ij} + \tilde{\mathbf{w}}_{ji}}{2}$ . For the update of  $\mathbf{Z}^{k+1}$ , we reconstruct the matrix  $\Theta = (\Theta_{ij})$  as

$$\Theta_{ij} = \frac{\alpha_1 \left\| \frac{\mathbf{h}_i}{\|\mathbf{h}_i\|} - \frac{\mathbf{h}_j}{\|\mathbf{h}_j\|} \right\|^2}{2\lambda \text{Tr}(\mathbf{H}\mathbf{L}_C\mathbf{H}^\top)} + \frac{\lambda_Z}{\lambda}. \quad (25)$$

The whole procedure of the alternating minimization scheme with normalization operations for (13) is given in Algorithm 3.

We denote the objective function of (13) as  $f(\mathbf{A}, \mathbf{Z}, \mathbf{H})$ . Let  $S_1 = \{\mathbf{Z} \mid \text{diag}(\mathbf{Z}) = \mathbf{0}\}$  and  $S_2 = \{\mathbf{H} \mid \mathbf{H}\mathbf{H}^\top =$

$\mathbf{I}\}$ , and we denote the indicator functions of  $S_1$  and  $S_2$  as  $\iota_{S_1}(\mathbf{Z})$  and  $\iota_{S_2}(\mathbf{H})$ . Then we give the convergence guarantee for Algorithm 2.

*Proposition 2: The sequence  $\{\mathbf{H}^k, \mathbf{A}^k, \mathbf{Z}^k\}$  generated by Algorithm 2 has the following properties:*

(1) The objective  $f(\mathbf{A}^k, \mathbf{Z}^k, \mathbf{H}^k) + \iota_{S_1}(\mathbf{Z}^k) + \iota_{S_2}(\mathbf{H}^k)$  is monotonically decreasing. Moreover,

$$\begin{aligned} & f(\mathbf{A}^{k+1}, \mathbf{Z}^{k+1}, \mathbf{H}^{k+1}) + \iota_{S_1}(\mathbf{Z}^{k+1}) + \iota_{S_2}(\mathbf{H}^{k+1}) \\ & \leq f(\mathbf{A}^k, \mathbf{Z}^k, \mathbf{H}^k) + \iota_{S_1}(\mathbf{Z}^k) + \iota_{S_2}(\mathbf{H}^k) \\ & \quad - \frac{\lambda}{2} \|\mathbf{A}^{k+1} - \mathbf{A}^k\|^2 - \frac{\lambda}{2} \|\mathbf{Z}^{k+1} - \mathbf{Z}^k\|^2; \end{aligned}$$

(2)  $\mathbf{A}^{k+1} - \mathbf{A}^k \rightarrow 0, \mathbf{Z}^{k+1} - \mathbf{Z}^k \rightarrow 0$ ;

(3) The sequences  $\{\mathbf{A}^k\}, \{\mathbf{Z}^k\}$  and  $\{\mathbf{H}^k\}$  are bounded.

*Theorem 1: The sequence  $\{\mathbf{A}^k, \mathbf{Z}^k, \mathbf{H}^k\}$  generated by Algorithm 2 has at least one limit point and any limit point  $(\mathbf{A}^*, \mathbf{Z}^*, \mathbf{H}^*)$  of  $\{\mathbf{A}^k, \mathbf{Z}^k, \mathbf{H}^k\}$  is a stationary point of (13).*

Please refer to the Appendix for the proofs of Theorem 1 and Proposition 2.

**Remark.** For Algorithm 2, the closed form solutions for  $\mathbf{A}^{k+1}$  and  $\mathbf{Z}^{k+1}$  can be obtained by (18) and (22). For the update of  $\mathbf{H}^{k+1}$ , the ALGORITHM 4.1 in [40] has been proven in [38] to converge globally to the optimal solution of (16).

### C. Complexity Analysis

Three sub-problems are included in Algorithm 3. The computation complexity of updating  $\mathbf{H}$  is  $O(\eta n^3)$ , where  $\eta$  is the maximum number of spectral decompositions to calculate  $\mathbf{H}$ . The computation complexity of updating  $\mathbf{A}$  is  $O(n^3)$ . The computation complexity of updating  $\mathbf{Z}$  is  $O(kn^2)$ . The computation complexity for the normalization operations is  $O(n^2)$ . Thus, the overall computation complexity of Algorithm 3 is  $O(T\eta n^3)$ , where  $T$  is the maximum number of iterations of alternating minimization. We set  $\eta = 20$  and  $T = 50$  in this paper.

In comparison, the compared methods CSP [24], SL [18] and LSGR [14] have computational complexity  $O(n^3)$ . CSCAP [20] has computation complexity  $O(n_c n^2 + n^3)$ , where  $n_c$  is the number of cannot-link constraints in  $\mathcal{C}$ . NNLR [41], S<sup>2</sup>LRR [26], S<sup>3</sup>R [26] and NNLR [25] have computational complexity  $O(Tn^3)$  while DCSSC [27] has computational complexity  $O(T(dn^2 + n^3))$ , where  $T$  is the total number of iterations.

## IV. EXPERIMENTS

In this section, we evaluate our proposed Dynamic Graph Structure Learning (DGSL) method by comparing the clustering performance of DGSL with state-of-the-art semi-supervised graph-based clustering methods on eight benchmark datasets.

### A. Experimental Settings

1) *Datasets:* Eight benchmark datasets including face images, handwritten digit images, object images and spoken letters are used in the experiments, i.e., Extended Yale B

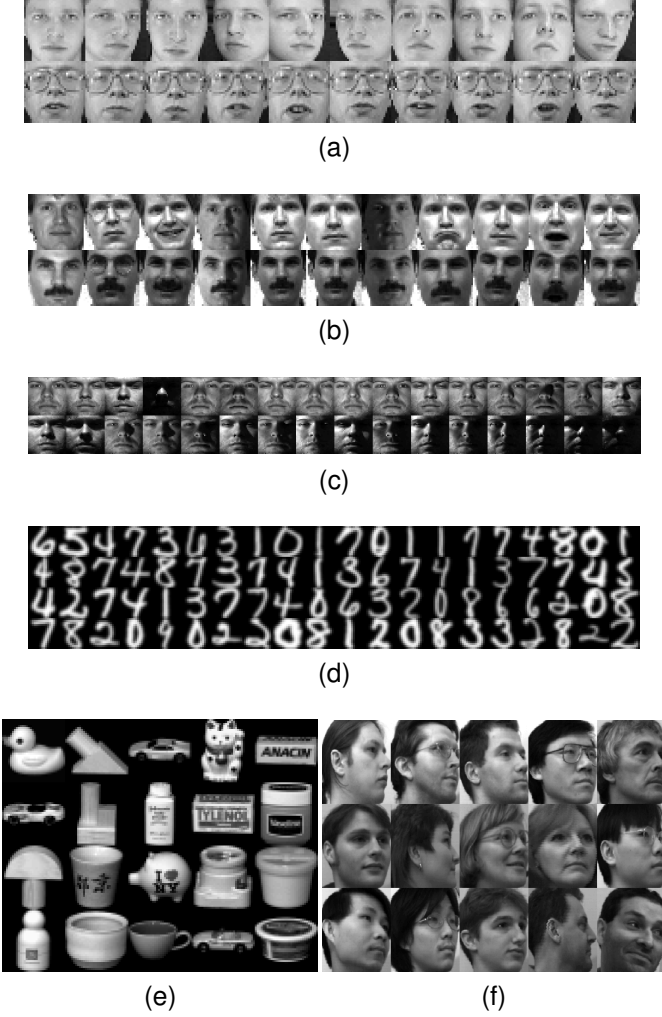


Fig. 2. Sample images of the datasets. (a) ORL. (b) Yale. (c) Extended Yale B. (d) USPS. (e) COIL20. (f) UMIST.

[42]<sup>1</sup>, Yale [43]<sup>2</sup>, COIL20<sup>3</sup>, UMIST<sup>4</sup>, Isolet [44]<sup>5</sup>, ORL [45]<sup>6</sup>, MNIST<sup>7</sup> and USPS<sup>8</sup>. Table I shows the important statistics of the datasets, and Fig. 2 shows sample images in these datasets.

- **ORL** contains 400 grayscale images of 40 individuals. The images are taken with different lighting conditions, facial expressions, and facial details. Each image is resized to  $32 \times 32$  pixels.
- **Yale** contains 165 grayscale images of 15 individuals. Images for each individual are taken with different facial expressions or configurations. Each image is resized to  $32 \times 32$  pixels.
- **MNIST** contains grayscale images of handwritten digits 0 ~ 9. Each image is of size  $28 \times 28$ . We randomly select 1000 images, with 100 images per digit.

- **USPS** contains 9,298 handwritten digit images. Each image is of size  $16 \times 16$ . We randomly select 1000 images, with 100 images per digit.
- **Extended Yale B** consists of 2,414 frontal face images of 38 individuals. Each image is downsampled to  $32 \times 32$  pixels. We follow the setting in [27]: the first 18 persons with 1,134 images are used in our experiments.
- **COIL20** consists of 1,440 images of 20 objects. The images of each object are taken five degrees apart as the object is rotated on a turntable. Each image is resized to  $32 \times 32$  pixels.
- **UMIST** contains 575 total images of 20 individuals. Each image is cropped into size  $112 \times 92$ .
- **Isolet** contains 150 speakers who spoke twice the name of each letter of the alphabet. The speakers are grouped into five sets, with 30 speakers in each set, denoted as isolet1 to isolet5.

TABLE I  
STATISTICS OF THE EIGHT DATASETS

Datasets	#Samples	#Dimensions	#Classes	Type
Yale	165	1,024	15	face
ORL	400	1,024	40	face
UMIST	575	10,304	20	face
MNIST	70,000	784	10	digit
USPS	9,298	256	10	digit
COIL20	1,440	1,024	20	object
Isolet	7,797	617	26	speech
Extended Yale B	2,414	1,024	38	face

2) *Compared Methods*: We compare the proposed DGSL with four state-of-the-art semi-supervised graph-based clustering methods that use pairwise constraints as supervision, i.e., SL [18], LSGR [14], CSCAP [20], CSP [24], and five state-of-the-art semi-supervised subspace clustering methods that use partial labels as supervision, i.e., NNLRs [41], NNLR [25], S<sup>3</sup>R [26], S<sup>2</sup>LRR [26], DCSSC [27].

3) *Evaluation Metrics*: For the clustering performance evaluation, we use two commonly used metrics [46], i.e., Accuracy (ACC) and Normalized Mutual Information (NMI). For the above two metrics, a higher value implies a better clustering performance.

4) *Implementation Details*: We first introduce how we decide the parameters in (13), i.e.,  $\alpha_1, \alpha_2, \lambda, \lambda_M$  and  $\lambda_Z$ . The parameter  $\lambda$  is fixed as a relatively large number, i.e.,  $\lambda = 100$ . The parameter  $\lambda_Z$  is tuned from  $\{0, 0.5, 1.0, 1.5, 2.0\}$ . For the parameter  $\alpha_1$ , we set  $\alpha_1 = 2\tau\lambda\text{Tr}(\mathbf{H}^1\mathbf{L}_C\mathbf{H}^{1\top})$ , where  $\mathbf{H}^1$  is obtained by solving (24) with  $\tilde{\mathbf{W}} = \mathbf{W} + \lambda_M\mathbf{M}$ , and we tune  $\tau$  from  $\{0.01, 0.02, 0.03, 0.05, 0.075, 0.1, 0.2, 0.3\}$ . We set  $\lambda_M = 10$  for most of datasets except  $\lambda_M = 100$  for Extended Yale B, COIL20 and UMIST,  $\lambda_M = 1$  for Isolet. For the parameter  $\alpha_2$ , we set  $\frac{\alpha_2}{\alpha_1} = 0.2$  for  $\lambda_M = 1, 10$  and  $\frac{\alpha_2}{\alpha_1} = 0.02$  for  $\lambda_M = 100$ . Then we introduce how we construct the affinity matrix  $\mathbf{W}$ . We set  $m = 7, l = 5$  for most of the datasets, except  $m = 51, l = 21$  for isolet1 and isolet2,  $m = 5, l = 3$  for UMIST, and  $m = 4, l = 3$  for Extended Yale B. For the grayscale images with grayscale values distributed in  $0 \sim 255$ , we normalize the grayscale values by dividing them by 255. To obtain the final clustering results, we conduct

<sup>1</sup><http://www.cad.zju.edu.cn/home/dengcai/Data/FaceData.html>

<sup>2</sup><http://www.cad.zju.edu.cn/home/dengcai/Data/FaceData.html>

<sup>3</sup><https://www.cs.columbia.edu/CAVE/software/softlib/coil-20.php>

<sup>4</sup><https://cs.nyu.edu/~roweis/data.html>

<sup>5</sup><http://www.cad.zju.edu.cn/home/dengcai/Data/MLData.html>

<sup>6</sup><http://www.cad.zju.edu.cn/home/dengcai/Data/FaceData.html>

<sup>7</sup><http://yann.lecun.com/exdb/mnist/>

<sup>8</sup><https://www.csie.ntu.edu.tw/~cjlin/libsvmtools/datasets/multiclass.html#usps>

TABLE II  
CLUSTERING PERFORMANCE (ACC%  $\pm$  STD%) ON DIFFERENT DATASETS

ACC	ORL			Yale			COIL20		
	2	3	4	2	3	4	2	6	10
SL [18]	66.8 $\pm$ 2.9	74.2 $\pm$ 2.2	81.7 $\pm$ 2.7	47.5 $\pm$ 2.8	55.2 $\pm$ 3.1	65.6 $\pm$ 3.3	71.0 $\pm$ 3.1	72.8 $\pm$ 3.3	76.2 $\pm$ 3.2
CSP [24]	78.4 $\pm$ 1.7	83.4 $\pm$ 5.1	87.5 $\pm$ 6.4	59.2 $\pm$ 1.8	61.4 $\pm$ 3.9	65.4 $\pm$ 3.4	80.0 $\pm$ 4.7	83.4 $\pm$ 5.1	87.7 $\pm$ 6.1
CSCAP [20]	82.3 $\pm$ 2.0	89.5 $\pm$ 2.4	92.3 $\pm$ 2.2	61.4 $\pm$ 3.3	65.4 $\pm$ 3.6	68.7 $\pm$ 3.0	70.9 $\pm$ 2.7	74.3 $\pm$ 2.9	76.0 $\pm$ 2.6
LSGR [14]	81.4 $\pm$ 2.8	86.4 $\pm$ 2.3	90.4 $\pm$ 1.9	63.2 $\pm$ 3.4	68.1 $\pm$ 2.9	73.6 $\pm$ 3.6	81.0 $\pm$ 1.4	82.4 $\pm$ 2.7	85.6 $\pm$ 1.0
DGSL	<b>90.4</b> $\pm$ 2.0	<b>94.5</b> $\pm$ 2.0	<b>96.4</b> $\pm$ 1.2	<b>64.8</b> $\pm$ 3.3	<b>73.5</b> $\pm$ 2.6	<b>80.0</b> $\pm$ 2.2	<b>85.1</b> $\pm$ 0.7	<b>93.4</b> $\pm$ 2.5	<b>97.2</b> $\pm$ 1.1
ACC	UMIST			isolet1			isolet2		
	2	3	4	5	7	10	5	7	10
SL [18]	82.4 $\pm$ 3.6	83.6 $\pm$ 4.1	83.7 $\pm$ 6.0	66.6 $\pm$ 1.1	67.5 $\pm$ 1.2	68.5 $\pm$ 1.4	63.3 $\pm$ 0.7	63.9 $\pm$ 0.6	65.0 $\pm$ 0.5
CSP [24]	84.3 $\pm$ 2.4	85.5 $\pm$ 1.9	85.8 $\pm$ 2.1	73.5 $\pm$ 2.7	74.9 $\pm$ 3.7	76.4 $\pm$ 4.5	70.0 $\pm$ 1.6	71.6 $\pm$ 2.0	72.8 $\pm$ 3.7
CSCAP [20]	82.9 $\pm$ 3.2	85.1 $\pm$ 4.0	87.2 $\pm$ 4.2	74.3 $\pm$ 1.6	75.4 $\pm$ 2.0	77.8 $\pm$ 1.4	67.8 $\pm$ 1.1	69.3 $\pm$ 2.0	70.5 $\pm$ 1.6
LSGR [14]	80.0 $\pm$ 1.5	81.8 $\pm$ 4.0	82.7 $\pm$ 5.9	69.7 $\pm$ 1.6	70.6 $\pm$ 1.5	72.7 $\pm$ 1.4	63.9 $\pm$ 0.9	65.0 $\pm$ 0.9	67.0 $\pm$ 1.2
DGSL	<b>89.1</b> $\pm$ 2.6	<b>92.5</b> $\pm$ 3.1	<b>94.3</b> $\pm$ 1.8	<b>82.9</b> $\pm$ 1.9	<b>86.4</b> $\pm$ 1.6	<b>89.1</b> $\pm$ 1.0	<b>74.4</b> $\pm$ 2.5	<b>79.8</b> $\pm$ 2.4	<b>83.6</b> $\pm$ 1.9
ACC	Extended Yale B			MNIST			USPS		
	4	7	10	5	7	10	5	7	10
SL [18]	87.0 $\pm$ 2.5	88.8 $\pm$ 2.2	90.3 $\pm$ 3.9	66.0 $\pm$ 3.9	69.8 $\pm$ 3.9	76.0 $\pm$ 5.6	84.3 $\pm$ 5.8	86.5 $\pm$ 5.7	87.6 $\pm$ 5.0
CSP [24]	87.8 $\pm$ 4.3	88.3 $\pm$ 4.2	88.8 $\pm$ 3.3	79.0 $\pm$ 4.0	83.2 $\pm$ 1.8	85.0 $\pm$ 1.5	88.2 $\pm$ 0.9	89.4 $\pm$ 0.9	90.7 $\pm$ 0.8
CSCAP [20]	88.0 $\pm$ 3.3	89.7 $\pm$ 3.4	90.7 $\pm$ 3.9	70.6 $\pm$ 5.0	72.7 $\pm$ 4.9	77.4 $\pm$ 4.6	86.1 $\pm$ 5.2	88.1 $\pm$ 4.5	89.8 $\pm$ 3.8
LSGR [14]	86.2 $\pm$ 3.3	88.2 $\pm$ 3.5	89.3 $\pm$ 2.5	67.1 $\pm$ 3.3	72.5 $\pm$ 5.5	76.6 $\pm$ 5.6	84.3 $\pm$ 5.6	85.5 $\pm$ 6.4	86.7 $\pm$ 5.4
DGSL	<b>95.4</b> $\pm$ 0.8	<b>95.6</b> $\pm$ 0.6	<b>96.4</b> $\pm$ 0.6	<b>83.7</b> $\pm$ 2.6	<b>86.2</b> $\pm$ 1.8	<b>88.6</b> $\pm$ 1.6	<b>91.5</b> $\pm$ 0.8	<b>92.3</b> $\pm$ 0.8	<b>93.0</b> $\pm$ 0.9

K-means on  $\{\frac{\mathbf{h}_i}{\|\mathbf{h}_i\|}\}_{i=1}^n$  for the output  $\mathbf{H} = [\mathbf{h}_1, \dots, \mathbf{h}_n]$  of Algorithm 3.

For the compared methods SL, CSP, LSGR, and CSCAP, one first needs to construct the affinity matrix. We construct the affinity matrix for MNIST, USPS, COIL20, isolet1, and isolet2 by (8) with the same setting of  $m$  and  $l$  as our approach. We construct the affinity matrix for ORL, Yale, UMIST, and Extended Yale B by first solving

$$\min_{\mathbf{A}, \mathbf{Z}} \frac{1}{2} \|\mathbf{X} - \mathbf{XA}\|^2 + \frac{\lambda}{2} \|\mathbf{A} - \mathbf{Z}\|^2 + \lambda_Z \|\mathbf{Z}\|_1 \text{ s.t. } \text{diag}(\mathbf{Z}) = \mathbf{0} \quad (26)$$

using alternating minimization, then we construct the  $i$ -th column of the affinity matrix as  $\frac{|\mathbf{z}_i|}{\|\mathbf{z}_i\|_\infty}$ ,  $i = 1, \dots, n$ . For LSGR, we report the best performance among the three types of semi-supervised spectral clustering algorithms in [14], i.e.,  $\mathcal{F}_{\text{ADJ}}$ ,  $\mathcal{F}_{\text{LAP}}$  and  $\mathcal{F}_{\text{NLAP}}$ , which are based on the affinity matrix, Laplacian matrix and normalized Laplacian matrix, respectively. For CSP, we report the performance of the constrained spectral clustering algorithm for  $K$ -way partition in [24]. For CSCAP, we report the performance of the constrained clustering algorithm for more than two classes in [20]. We normalize the obtained low-dimensional representations of data points into unit Euclidean length before K-means clustering for the four compared methods that use pairwise constraints as supervisory information.

### B. Comparisons with Methods That Use Pairwise Constraints as Supervisory Information

We compare our proposed DGSL with four state-of-the-art semi-supervised graph-based clustering methods which use pairwise constraints as supervisory information, i.e., SL [18], LSGR [14], CSCAP [20], CSP [24]. We use two different settings to generate the pairwise constraints. In the first setting,

for any class  $i$ , we randomly select a subset of data points, denoted as  $S_i$ , to construct the supervisory information. Then the set of must-link constraints  $\mathcal{M}$  is defined as  $\mathcal{M} = \{(\mathbf{x}_i, \mathbf{x}_j) | \mathbf{x}_i \in S_k, \mathbf{x}_j \in S_t, k = t\}$ , and the set of cannot-link constraints  $\mathcal{C}$  is defined as  $\mathcal{C} = \{(\mathbf{x}_i, \mathbf{x}_j) | \mathbf{x}_i \in S_k, \mathbf{x}_j \in S_t, k \neq t\}$ . In the second setting, we randomly choose different numbers of data pairs with the same class label to generate  $\mathcal{M}$  and data pairs with different class labels to generate  $\mathcal{C}$ .

For the first setting, we choose  $f$  data points to construct  $S_i$  for any class  $i$ , e.g.,  $f = 2, 3, 4$  for ORL dataset. Each experiment is repeated 20 times independently with different supervisory information, and we report the average results, i.e., ACC (%) and NMI (%), as well as the standard deviations (STD%). The clustering results are shown in Table II and Table III. The best results are in bold font.

For the second setting, we set the number of cannot-link constraints as three times the number of must-link constraints. Each experiment is repeated 20 times with different supervisory information, and we report the average results in Fig. 3.

From Table II, Table III and Fig. 3, the following observations can be made: (1) DGSL consistently achieves the highest ACC and NMI on most datasets, which verifies the effectiveness of our dynamic graph structure learning scheme; (2) The performance of our proposed DGSL improves rapidly with the increasing supervisory information on most datasets, demonstrating that DGSL can utilize the supervisory information effectively.

### C. Comparisons with Methods That Use Partial Labels as Supervisory Information

We also compare DGSL with five state-of-the-art semi-supervised subspace clustering methods that use partial labels as supervisory information, i.e., NNLS [41], NNLR

TABLE III  
CLUSTERING PERFORMANCE (NMI%  $\pm$  STD%) ON DIFFERENT DATASETS

NMI	ORL			Yale			COIL20		
	2	3	4	2	3	4	2	6	10
SL [18]	83.5 $\pm$ 1.2	87.6 $\pm$ 1.1	91.6 $\pm$ 1.3	53.7 $\pm$ 2.0	60.5 $\pm$ 2.7	68.9 $\pm$ 2.4	87.3 $\pm$ 1.6	87.7 $\pm$ 1.3	89.0 $\pm$ 1.3
CSP [24]	89.5 $\pm$ 0.8	88.9 $\pm$ 3.5	91.7 $\pm$ 4.1	62.7 $\pm$ 1.8	64.4 $\pm$ 3.0	67.5 $\pm$ 2.9	89.1 $\pm$ 1.6	91.5 $\pm$ 1.6	92.3 $\pm$ 2.2
CSCAP [20]	90.9 $\pm$ 0.7	94.1 $\pm$ 1.1	95.2 $\pm$ 1.3	63.3 $\pm$ 3.0	66.8 $\pm$ 2.6	70.1 $\pm$ 2.6	86.8 $\pm$ 1.3	87.8 $\pm$ 1.7	88.9 $\pm$ 1.4
LSGR [14]	90.8 $\pm$ 1.1	93.5 $\pm$ 0.9	95.6 $\pm$ 0.7	<b>65.9</b> $\pm$ 2.5	70.4 $\pm$ 2.3	75.6 $\pm$ 2.4	92.0 $\pm$ 0.8	93.1 $\pm$ 0.9	94.3 $\pm$ 0.7
DGSL	<b>94.1</b> $\pm$ 0.9	<b>96.3</b> $\pm$ 1.1	<b>97.4</b> $\pm$ 0.8	64.7 $\pm$ 2.8	<b>71.2</b> $\pm$ 2.5	<b>77.4</b> $\pm$ 2.1	<b>94.7</b> $\pm$ 0.7	<b>96.9</b> $\pm$ 0.7	<b>97.4</b> $\pm$ 0.7
NMI	UMIST			isolet1			isolet2		
	2	3	4	5	7	10	5	7	10
SL [18]	87.5 $\pm$ 1.8	88.7 $\pm$ 1.8	89.7 $\pm$ 2.3	78.6 $\pm$ 0.3	79.1 $\pm$ 0.5	79.9 $\pm$ 0.5	75.5 $\pm$ 0.7	76.0 $\pm$ 0.5	76.9 $\pm$ 0.6
CSP [24]	88.1 $\pm$ 1.3	88.7 $\pm$ 0.9	89.0 $\pm$ 1.2	82.3 $\pm$ 0.6	83.2 $\pm$ 0.7	84.2 $\pm$ 0.9	80.3 $\pm$ 0.6	81.3 $\pm$ 0.8	82.7 $\pm$ 0.7
CSCAP [20]	87.9 $\pm$ 1.6	89.3 $\pm$ 1.6	91.0 $\pm$ 1.8	80.6 $\pm$ 0.7	81.9 $\pm$ 0.6	83.2 $\pm$ 0.9	78.0 $\pm$ 0.5	78.5 $\pm$ 0.6	79.3 $\pm$ 0.7
LSGR [14]	85.1 $\pm$ 0.8	88.5 $\pm$ 1.7	89.9 $\pm$ 2.1	79.0 $\pm$ 0.6	79.7 $\pm$ 0.7	81.0 $\pm$ 0.6	75.2 $\pm$ 0.5	76.0 $\pm$ 0.4	76.8 $\pm$ 0.4
DGSL	<b>93.3</b> $\pm$ 1.0	<b>94.9</b> $\pm$ 1.0	<b>95.6</b> $\pm$ 1.0	<b>85.6</b> $\pm$ 0.7	<b>87.1</b> $\pm$ 0.9	<b>88.7</b> $\pm$ 0.7	<b>81.6</b> $\pm$ 1.0	<b>83.5</b> $\pm$ 1.1	<b>85.3</b> $\pm$ 0.9
NMI	Extended Yale B			MNIST			USPS		
	4	7	10	5	7	10	5	7	10
SL [18]	90.5 $\pm$ 0.7	91.2 $\pm$ 0.8	91.9 $\pm$ 1.1	66.7 $\pm$ 1.9	69.2 $\pm$ 1.6	72.9 $\pm$ 2.3	80.1 $\pm$ 2.1	81.6 $\pm$ 2.3	83.0 $\pm$ 1.7
CSP [24]	90.3 $\pm$ 1.6	90.5 $\pm$ 1.8	91.0 $\pm$ 1.3	71.2 $\pm$ 2.5	73.0 $\pm$ 1.9	75.0 $\pm$ 1.8	79.9 $\pm$ 1.0	81.4 $\pm$ 1.1	83.3 $\pm$ 1.0
CSCAP [20]	89.9 $\pm$ 1.1	89.6 $\pm$ 1.0	91.6 $\pm$ 1.1	69.4 $\pm$ 2.6	70.4 $\pm$ 2.2	74.0 $\pm$ 2.7	80.8 $\pm$ 2.1	82.1 $\pm$ 2.1	84.0 $\pm$ 1.4
LSGR [14]	89.2 $\pm$ 1.1	90.2 $\pm$ 1.1	91.1 $\pm$ 1.0	67.4 $\pm$ 1.6	69.9 $\pm$ 2.2	73.6 $\pm$ 2.4	80.4 $\pm$ 2.2	81.7 $\pm$ 2.0	82.9 $\pm$ 1.8
DGSL	<b>93.4</b> $\pm$ 0.9	<b>93.6</b> $\pm$ 0.7	<b>94.6</b> $\pm$ 0.7	<b>76.6</b> $\pm$ 1.5	<b>78.6</b> $\pm$ 1.6	<b>80.6</b> $\pm$ 1.5	<b>85.4</b> $\pm$ 0.8	<b>86.3</b> $\pm$ 1.0	<b>87.2</b> $\pm$ 1.0

TABLE IV  
CLUSTERING PERFORMANCE (ACC%  $\pm$  STD%) ON DIFFERENT DATASETS

ACC	COIL20			Extended Yale B			Yale		
	2	6	10	4	7	10	2	3	4
Using Partial Labels as Supervision									
NNLRS [41]	74.9 $\pm$ 3.0	84.5 $\pm$ 2.8	89.4 $\pm$ 3.0	75.5 $\pm$ 2.6	84.8 $\pm$ 2.0	89.0 $\pm$ 3.0	56.7 $\pm$ 3.5	67.0 $\pm$ 4.1	71.8 $\pm$ 3.6
S <sup>2</sup> LRR [26]	50.2 $\pm$ 6.9	80.0 $\pm$ 2.5	84.2 $\pm$ 2.3	93.3 $\pm$ 0.8	93.7 $\pm$ 0.7	95.5 $\pm$ 0.4	60.5 $\pm$ 4.2	72.5 $\pm$ 5.1	75.7 $\pm$ 4.8
S <sup>3</sup> R [26]	79.4 $\pm$ 4.0	88.3 $\pm$ 3.5	92.8 $\pm$ 0.3	87.8 $\pm$ 4.7	92.2 $\pm$ 2.4	92.7 $\pm$ 1.4	58.9 $\pm$ 6.6	68.5 $\pm$ 5.1	70.5 $\pm$ 4.4
NNLRR [25]	76.4 $\pm$ 4.7	88.5 $\pm$ 1.2	91.3 $\pm$ 1.2	72.0 $\pm$ 1.7	85.6 $\pm$ 2.0	88.0 $\pm$ 0.8	58.6 $\pm$ 3.1	67.8 $\pm$ 3.6	73.8 $\pm$ 3.4
DCSSC [27]	79.4 $\pm$ 3.6	<b>94.3</b> $\pm$ 0.7	94.9 $\pm$ 0.2	93.2 $\pm$ 0.9	95.5 $\pm$ 0.9	<b>97.1</b> $\pm$ 0.6	<b>66.7</b> $\pm$ 2.3	<b>74.6</b> $\pm$ 3.2	<b>80.0</b> $\pm$ 1.3
Using Pairwise Constraints as Supervision									
DGSL	<b>85.1</b> $\pm$ 0.7	93.4 $\pm$ 2.5	<b>97.2</b> $\pm$ 1.1	<b>95.4</b> $\pm$ 0.8	<b>95.6</b> $\pm$ 0.6	96.4 $\pm$ 0.6	64.8 $\pm$ 3.3	73.5 $\pm$ 2.6	<b>80.0</b> $\pm$ 2.2

[25], S<sup>3</sup>R [26], S<sup>2</sup>LRR [26] and DCSSC [27]. We randomly select  $f$  data points from any class  $i$ , denoted as  $S_i$ , as labeled samples to generate the supervisory information, e.g.,  $f = 2, 6, 10$  for COIL20 dataset. The clustering performance of compared methods is cited from literature in [27]. The clustering performance is shown in Table IV and the best results are in bold font. It can be seen that our proposed DGSL achieves competitive results on the three datasets. Specifically, DGSL achieves at least 5.7% improvement over ACC of the compared methods for the case  $f = 2$  in the COIL20 dataset. Thus, for datasets COIL20, Yale, and Extended Yale B, DGSL can achieve competitive clustering performance compared with state-of-the-art semi-supervised subspace clustering methods. Moreover, DGSL adopts weaker and more flexible supervisory information, i.e., pairwise constraints, than the compared methods that leverage partial labels.

#### D. Experiments on Incomplete Labeled Classes

To further verify that our proposed DGSL can utilize the supervisory information effectively, we conduct experiments

on generating pairwise constraints with incomplete labeled classes. For each dataset,  $k_0$  labeled classes are chosen. For any chosen class  $i$ , we randomly select  $f$  data points, denoted as  $S_i$ , to generate the pairwise constraints. Then we define the pairwise constraints,  $\mathcal{M} = \{(\mathbf{x}_i, \mathbf{x}_j) | \mathbf{x}_i \in S_k, \mathbf{x}_j \in S_t, k = t\}$  and  $\mathcal{C} = \{(\mathbf{x}_i, \mathbf{x}_j) | \mathbf{x}_i \in S_k, \mathbf{x}_j \in S_t, k \neq t\}$ . We set  $f$  as 2, 2, 5, and 5 for the datasets ORL, Yale, MNIST, and isolet1, respectively. Then we choose  $k_0$  as 20%, 40%, 60%, 80% and 100% of the total number of classes for each dataset. Each experiment is repeated 20 times with different supervisory information, and we report the average results in Fig. 4. The following observations can be made: (1) The performance of DGSL improves rapidly on datasets ORL, MNIST, and isolet1, with the increasing of the number of labeled classes  $k_0$ . It further demonstrates that DGSL can utilize the supervisory information effectively; (2) DGSL achieves higher ACC and NMI than the compared methods in most cases, which further verifies the effectiveness of our approach.



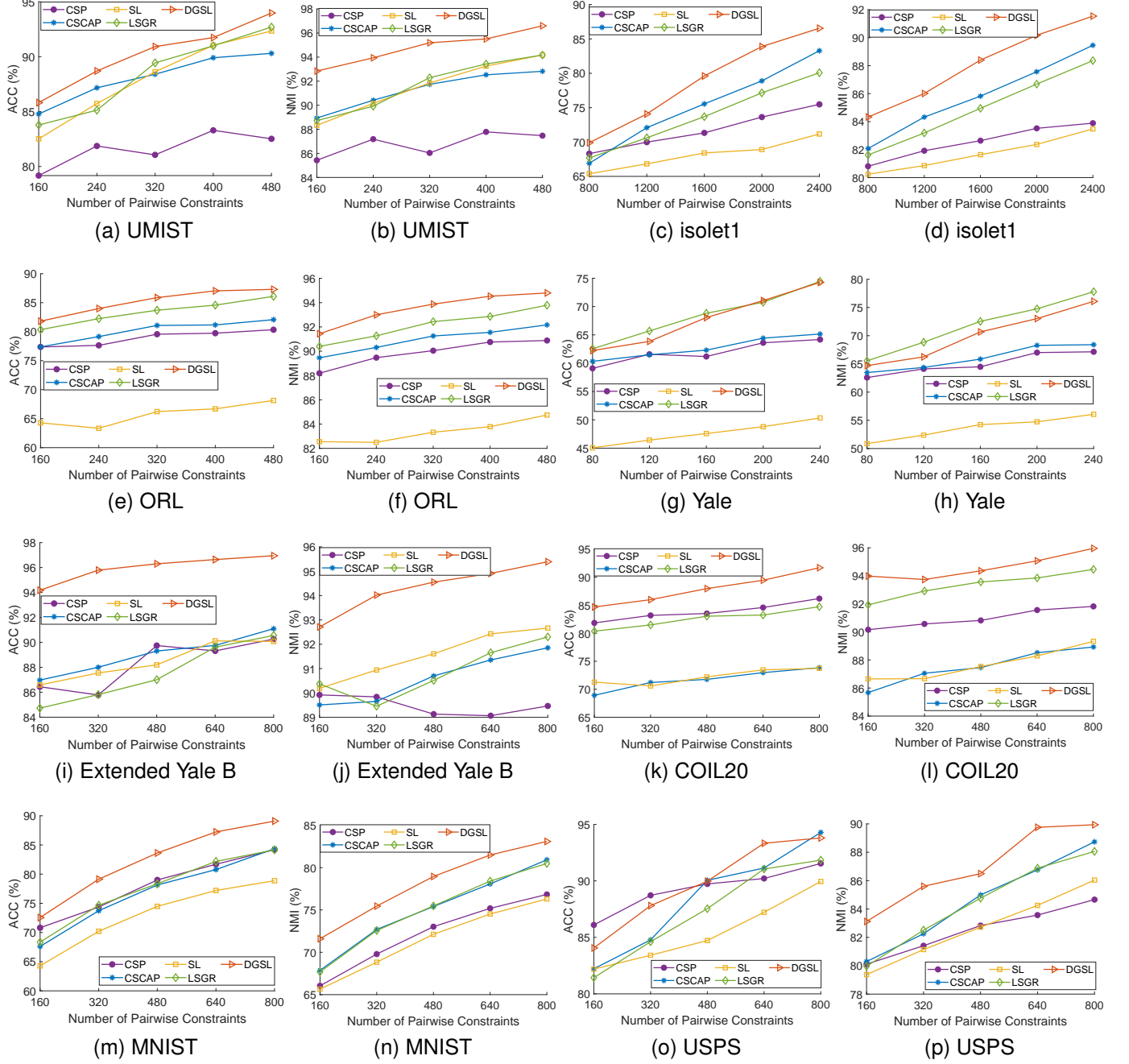


Fig. 3. Clustering performance on different datasets with different numbers of pairwise constraints.

### E. Parameters Sensitivity Study

Our proposed DGSL introduces five parameters, i.e.,  $\alpha_1, \alpha_2, \lambda, \lambda_M$  and  $\lambda_Z$  to control the ratio of different components. Since we fix  $\lambda = 100$ , we study the effect of parameters  $\alpha_1, \alpha_2, \lambda_M$  and  $\lambda_Z$  in this section. We generate the pairwise constraints by the first setting in Section IV-B and set  $f$  as 2, 2, 5 and 5 for ORL, Yale, MNIST and isolet1, respectively. We fix all other parameters except the tested one and show the results in Fig. 5. For parameter  $\alpha_1$ , we set  $\alpha_1 = 2\tau\lambda\text{Tr}(\mathbf{H}^1\mathbf{L}_C\mathbf{H}^{1\top})$  and tune  $\tau$  from  $\{0.01, 0.02, 0.03, 0.05, 0.075, 0.1, 0.2, 0.3\}$ . From Fig. 5, the following observations can be made: (1) The parameter  $\alpha_1$

is relatively vital to the clustering performance. Thus the regularization term  $\text{Tr}(\mathbf{H}\mathbf{L}_Z\mathbf{H}^\top)$  plays an important role in the reciprocal learning of  $\mathbf{H}$  and  $\mathbf{Z}$ ; (2) The clustering performance of DGSL is robust to the change of the parameter  $\alpha_2$ . Moreover,  $\frac{\alpha_2}{\alpha_1} = 0.2$  is a good choice; (3) The clustering performance of DGSL on datasets ORL, Yale and MNIST is robust to the parameters  $\lambda_M$  and  $\lambda_Z$  where  $\lambda_M = 10$  is a good choice for these three datasets; (4) The metric NMI is more robust to the metric ACC for the four parameters.

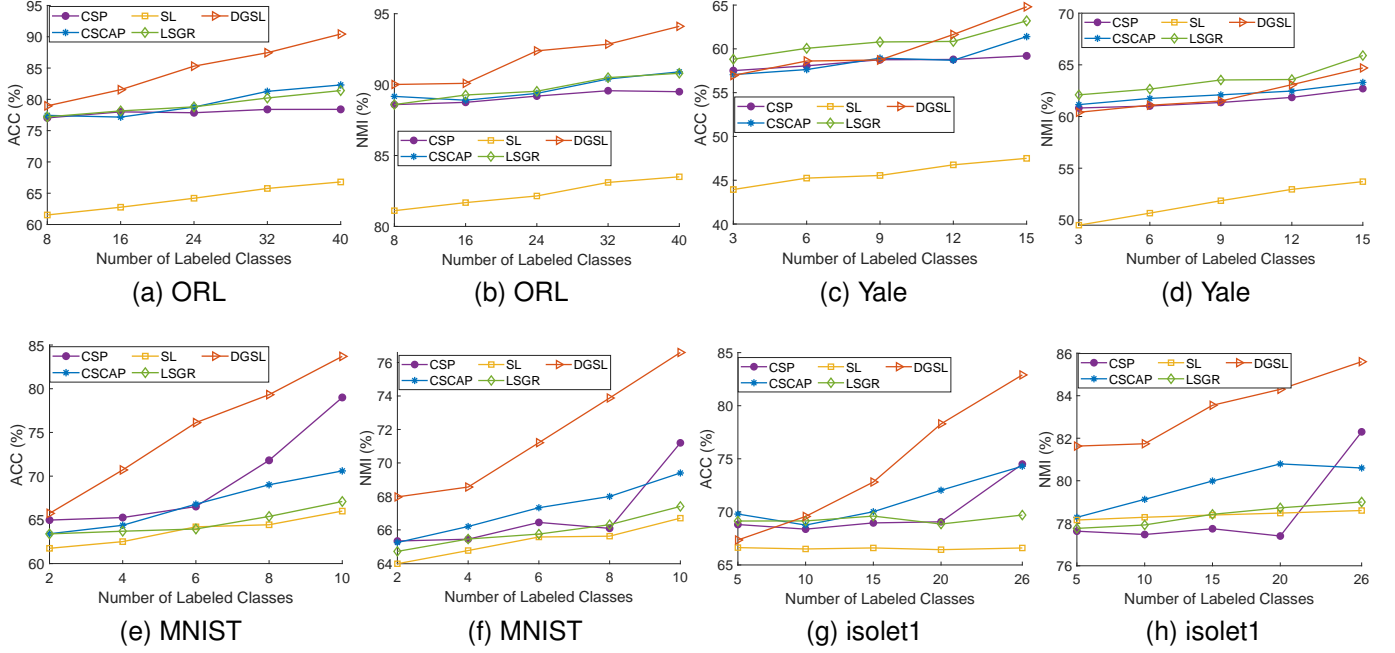


Fig. 4. Clustering performance on different datasets with different numbers of labeled classes.

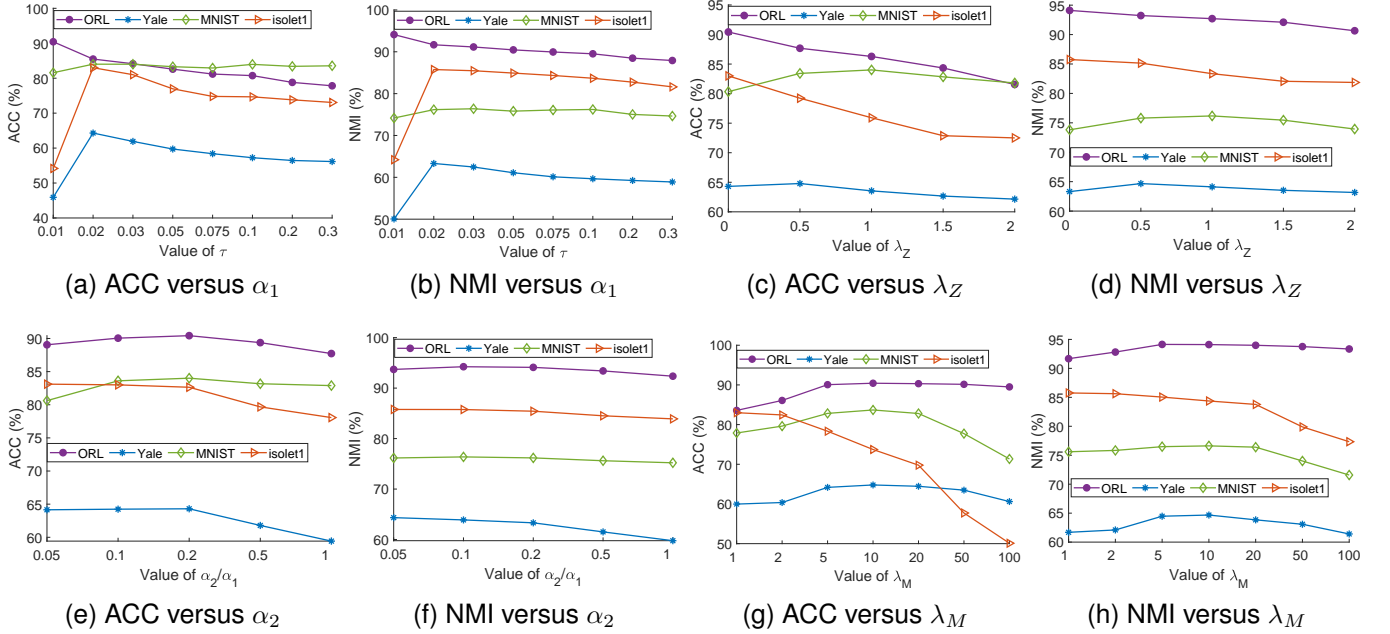


Fig. 5. Clustering performance of our method on different datasets with different values of the parameters  $\alpha_1$ ,  $\lambda_Z$ ,  $\alpha_2$  and  $\lambda_M$ .

### F. Visualization of Representation and Affinity

We plot the affinity matrix  $|\mathbf{Z}|$  and the distance matrix  $\mathbf{P}$  of the low-dimensional representations  $\mathbf{H}$  at the first iteration and the 30th iteration in Algorithm 3, as shown in Fig. 6. The first setting of pairwise constraints in Section IV-B is used. We set  $f$  as 2 for the ORL dataset. From Fig. 6, we can observe that the affinity matrix  $|\mathbf{Z}|$  and the distance matrix  $\mathbf{P}$  have a clear block diagonal structure at the 30th iteration, which means that the intra-class distance is small and the inter-class distance is relatively large for  $\mathbf{H}$  while the intra-class affinity

is high and the inter-class affinity is low for  $|\mathbf{Z}|$ . Thus the low-dimensional representations  $\mathbf{H}$  and the affinity matrix  $|\mathbf{Z}|$  are mutually refined during the iteration process.

### G. Experiments on Datasets with Hypergraph Structure

A hypergraph includes a vertex set  $\mathcal{V}$  and a hyperedge set  $\mathcal{E}$ . Each hyperedge  $e$  is a subset of  $\mathcal{V}$  associated with a positive weight  $w(e)$ . The hypergraph structure can be represented by a  $|\mathcal{V}| \times |\mathcal{E}|$  incidence matrix  $\mathbf{U}$ , with elements  $\mathbf{U}(v, e) = 1$  if  $v \in e$  and 0 otherwise. The degree of a vertex  $v$  is defined as

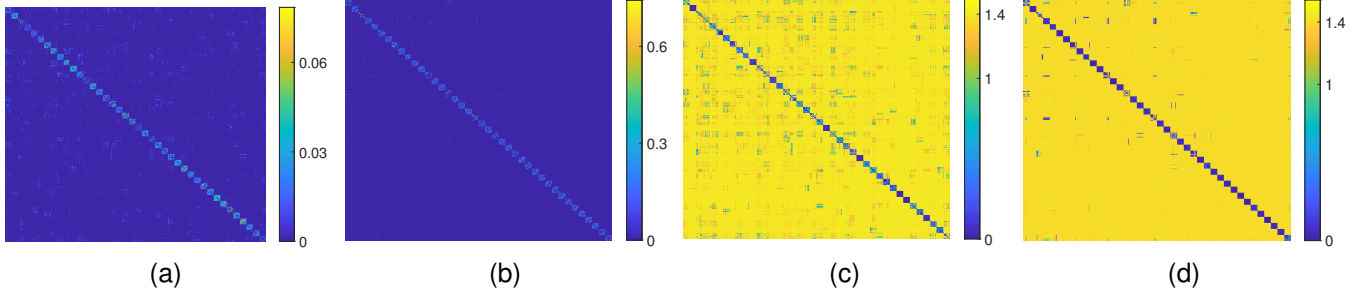


Fig. 6. Plots of matrices in Algorithm 3 for ORL dataset. (a)  $|Z^k|$ ,  $k=1$ . (b)  $|Z^k|$ ,  $k=30$ . (c) Distance matrix  $P^k$ , with  $P_{ij}^k = \frac{\|h_i\|}{\|h_i\| + \|h_j\|}$ ,  $k=1$ . (d) Distance matrix  $P^k$ , with  $P_{ij}^k = \frac{\|h_i\|}{\|h_i\| + \|h_j\|}$ ,  $k=30$ .

$d(v) = \sum_{e \in \mathcal{E}} \omega(e) \mathbf{U}(v, e)$  and the degree of a hyperedge  $e$  is defined as  $\delta(e) = \sum_{v \in \mathcal{V}} \mathbf{U}(v, e)$ . We denote  $\mathbf{D}_e$ ,  $\mathbf{D}_v$  and  $\mathbf{W}_e$  as the diagonal matrices containing the hyperedge degrees, the vertex degrees, and the hyperedge weights, respectively. Then the hypergraph Laplacian is defined as  $\Delta = \mathbf{I} - \mathbf{O}$ , where  $\mathbf{O} = \mathbf{D}_v^{-1/2} \mathbf{U} \mathbf{W}_e \mathbf{D}_e^{-1} \mathbf{U}^\top \mathbf{D}_v^{-1/2}$ .

We conduct experiments on the dataset Cora [47] and construct the hypergraph following the setting in [48]: each hyperedge is built by linking one vertex and their neighbors according to the adjacency relation on the graph. For the compared methods SL [18], CSP [24], CSCAP [20] and LSGR [14], we construct the affinity matrix as  $\mathbf{W} + \gamma_2 \mathbf{O}$ , where  $\mathbf{W}$  is defined in (8) and we set  $m = 7, l = 5$  for the construction of  $\mathbf{W}$ . For our proposed DGSL, we substitute  $\mathbf{W}$  in (13) by  $\mathbf{W} + \gamma_2 \mathbf{O}$ . We also compare with two state-of-the-art hypergraph learning methods, i.e., HI [49] and HGNN [48], and we follow the setting in [48] to generate the labeled data and the test data. The clustering performance is shown in Fig. 7. From Fig. 7, it can be observed that our proposed DGSL can achieve competitive clustering accuracy compared with the state-of-the-art hypergraph learning method. Moreover, DGSL adopts weaker and more flexible supervisory information, i.e., pairwise constraints, than HGNN which adopts partial labels as supervision.

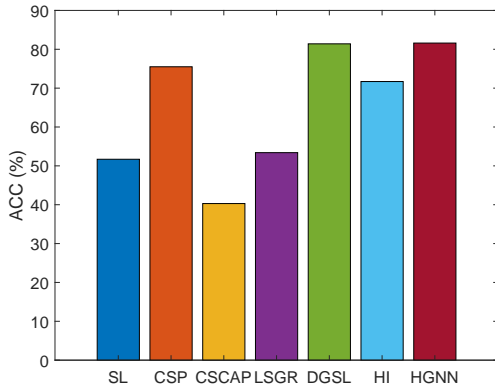


Fig. 7. Clustering performance (ACC%) on the Cora dataset.

## V. CONCLUSION

We propose a novel dynamic graph structure learning method for semi-supervised clustering. In this method, we

simultaneously optimize the graph structure and the low-dimensional representations of data points in a unified optimization framework. Moreover, we construct the graph structure by integrating the local distance and global self-representation among data points. An alternating minimization scheme is proposed to solve the unified optimization framework with proven convergence. Extensive experiments are conducted on eight benchmark datasets, including face images, object images, spoken letters, and handwritten digits, to demonstrate the effectiveness of our approach. Furthermore, we extend our approach to a benchmark hypergraph dataset and achieve competitive performance compared with state-of-the-art hypergraph learning methods.

## APPENDIX

*Proof of Proposition 1:* Note that  $\mathbf{L}_S = \mathbf{D}_S - \frac{|\mathbf{S}| + |\mathbf{S}|^\top}{2}$ , where  $\mathbf{D}_S$  is a diagonal matrix with the  $i$ -th diagonal element being  $\sum_{j=1}^n \frac{|s_{ij}| + |s_{ji}|}{2}$ . Then we can derive that

$$\begin{aligned}
 & \text{Tr}(\mathbf{H} \mathbf{L}_S \mathbf{H}^\top) \\
 &= \text{Tr}(\mathbf{H} \mathbf{D}_S \mathbf{H}^\top) - \text{Tr}\left(\mathbf{H} \left(\frac{|\mathbf{S}| + |\mathbf{S}|^\top}{2}\right) \mathbf{H}^\top\right) \\
 &= \sum_{i=1}^n \left( \sum_{j=1}^n \frac{|s_{ij}| + |s_{ji}|}{2} \right) \|\mathbf{h}_i\|^2 - \sum_{i,j=1}^n \frac{|s_{ij}| + |s_{ji}|}{2} \mathbf{h}_i^\top \mathbf{h}_j \\
 &= \frac{1}{2} \sum_{i,j=1}^n \frac{|s_{ij}| + |s_{ji}|}{2} (\|\mathbf{h}_i\|^2 + \|\mathbf{h}_j\|^2) - \sum_{i,j=1}^n \frac{|s_{ij}| + |s_{ji}|}{2} \mathbf{h}_i^\top \mathbf{h}_j \\
 &= \frac{1}{2} \sum_{i,j=1}^n \frac{|s_{ij}| + |s_{ji}|}{2} (\|\mathbf{h}_i - \mathbf{h}_j\|^2) \\
 &= \frac{1}{2} \sum_{i,j=1}^n |s_{ij}| \|\mathbf{h}_i - \mathbf{h}_j\|^2.
 \end{aligned} \tag{27}$$

The proof is completed.  $\blacksquare$

*Proof of Proposition 2:* We follow the proof of Proposition 8 in [34]. From the updating rule of  $\mathbf{H}^{k+1}$  in (14), we can obtain

$$f(\mathbf{A}^k, \mathbf{Z}^k, \mathbf{H}^{k+1}) + \iota_{S_2}(\mathbf{H}^{k+1}) \leq f(\mathbf{A}^k, \mathbf{Z}^k, \mathbf{H}^k) + \iota_{S_2}(\mathbf{H}^k). \tag{28}$$

From the updating rule of  $\mathbf{A}^{k+1}$  in (17), we can obtain

$$\mathbf{A}^{k+1} = \arg \min_{\mathbf{A}} f(\mathbf{A}, \mathbf{Z}^k, \mathbf{H}^{k+1}). \tag{29}$$

Note that  $f(\mathbf{A}, \mathbf{Z}^k, \mathbf{H}^{k+1})$  is  $\lambda$ -strongly convex w.r.t.  $\mathbf{A}$ . We can obtain

$$f(\mathbf{A}^{k+1}, \mathbf{Z}^k, \mathbf{H}^{k+1}) \leq f(\mathbf{A}^k, \mathbf{Z}^k, \mathbf{H}^{k+1}) - \frac{\lambda}{2} \|\mathbf{A}^{k+1} - \mathbf{A}^k\|^2 \quad (30)$$

where we use the Lemma B.5 in [50]. Similarly, note that  $f(\mathbf{A}^{k+1}, \mathbf{Z}, \mathbf{H}^{k+1}) + \iota_{S_1}(\mathbf{Z})$  is  $\lambda$ -strongly convex w.r.t.  $\mathbf{Z}$ . We can obtain

$$\begin{aligned} & f(\mathbf{A}^{k+1}, \mathbf{Z}^{k+1}, \mathbf{H}^{k+1}) + \iota_{S_1}(\mathbf{Z}^{k+1}) \\ & \leq f(\mathbf{A}^{k+1}, \mathbf{Z}^k, \mathbf{H}^{k+1}) + \iota_{S_1}(\mathbf{Z}^k) - \frac{\lambda}{2} \|\mathbf{Z}^{k+1} - \mathbf{Z}^k\|^2. \end{aligned} \quad (31)$$

Integrating (28), (30) and (31), we can obtain

$$\begin{aligned} & f(\mathbf{A}^{k+1}, \mathbf{Z}^{k+1}, \mathbf{H}^{k+1}) + \iota_{S_1}(\mathbf{Z}^{k+1}) + \iota_{S_2}(\mathbf{H}^{k+1}) \\ & \leq f(\mathbf{A}^k, \mathbf{Z}^k, \mathbf{H}^k) + \iota_{S_1}(\mathbf{Z}^k) + \iota_{S_2}(\mathbf{H}^k) \\ & \quad - \frac{\lambda}{2} \|\mathbf{Z}^{k+1} - \mathbf{Z}^k\|^2 - \frac{\lambda}{2} \|\mathbf{A}^{k+1} - \mathbf{A}^k\|^2. \end{aligned} \quad (32)$$

Note that  $f(\mathbf{A}^k, \mathbf{Z}^k, \mathbf{H}^k) + \iota_{S_1}(\mathbf{Z}^k) + \iota_{S_2}(\mathbf{H}^k) \geq 0$ . Now, summing (32) over  $k = 0, 1, \dots$ , we can obtain

$$\sum_{k=0}^{+\infty} \frac{\lambda}{2} (\|\mathbf{Z}^{k+1} - \mathbf{Z}^k\|^2 + \|\mathbf{A}^{k+1} - \mathbf{A}^k\|^2) \leq f(\mathbf{A}^0, \mathbf{Z}^0, \mathbf{H}^0). \quad (33)$$

This implies

$$\mathbf{Z}^{k+1} - \mathbf{Z}^k \rightarrow 0, \quad (34)$$

$$\mathbf{A}^{k+1} - \mathbf{A}^k \rightarrow 0. \quad (35)$$

From (32),  $f(\mathbf{A}^k, \mathbf{Z}^k, \mathbf{H}^k) + \iota_{S_1}(\mathbf{Z}^k) + \iota_{S_2}(\mathbf{H}^k)$  is monotonically decreasing and thus it is upper bounded. From the expression of  $f(\mathbf{A}^k, \mathbf{Z}^k, \mathbf{H}^k)$ , it is easy to see that  $\{\|\mathbf{Z}^k\|_1\}$  and  $\{\|\mathbf{A}^k - \mathbf{Z}^k\|^2\}$  are bounded. Then  $\{\mathbf{A}^k\}$  and  $\{\mathbf{Z}^k\}$  are bounded. Also,  $\mathbf{H}^k \in S_2$  implies that  $\mathbf{H}^k \mathbf{H}^{k\top} = \mathbf{I}$  and thus  $\{\mathbf{H}^k\}$  is bounded. The proof is completed. ■

*Proof of Theorem 1:* From the boundedness of  $\{\mathbf{A}^k, \mathbf{Z}^k, \mathbf{H}^k\}$ , there exists a point  $(\mathbf{A}^*, \mathbf{Z}^*, \mathbf{H}^*)$  and a subsequence  $\{\mathbf{A}^{k_j+1}, \mathbf{Z}^{k_j+1}, \mathbf{H}^{k_j+1}\}$  such that  $\mathbf{A}^{k_j+1} \rightarrow \mathbf{A}^*$ ,  $\mathbf{Z}^{k_j+1} \rightarrow \mathbf{Z}^*$  and  $\mathbf{H}^{k_j+1} \rightarrow \mathbf{H}^*$ . Then by (34) and (35), we have  $\mathbf{A}^{k_j} \rightarrow \mathbf{A}^*$ ,  $\mathbf{Z}^{k_j} \rightarrow \mathbf{Z}^*$ . On the other hand, from the optimality of  $\mathbf{H}^{k_j+1}$  for (14),  $\mathbf{A}^{k_j+1}$  for (17),  $\mathbf{Z}^{k_j+1}$  for (19), we have

$$f(\mathbf{A}^{k_j}, \mathbf{Z}^{k_j}, \mathbf{H}^{k_j+1}) + \iota_{S_2}(\mathbf{H}^{k_j+1}) \quad (36)$$

$$\leq f(\mathbf{A}^{k_j}, \mathbf{Z}^{k_j}, \mathbf{H}) + \iota_{S_2}(\mathbf{H}), \forall \mathbf{H} \quad (37)$$

$$f(\mathbf{A}^{k_j+1}, \mathbf{Z}^{k_j}, \mathbf{H}^{k_j+1}) \leq f(\mathbf{A}, \mathbf{Z}^{k_j}, \mathbf{H}^{k_j+1}), \forall \mathbf{A} \quad (38)$$

$$f(\mathbf{A}^{k_j+1}, \mathbf{Z}^{k_j+1}, \mathbf{H}^{k_j+1}) + \iota_{S_1}(\mathbf{Z}^{k_j+1}) \quad (39)$$

$$\leq f(\mathbf{A}^{k_j+1}, \mathbf{Z}, \mathbf{H}^{k_j+1}) + \iota_{S_1}(\mathbf{Z}), \forall \mathbf{Z} \quad (40)$$

Let  $k_j \rightarrow +\infty$  in (36)-(40). We can obtain

$$f(\mathbf{A}^*, \mathbf{Z}^*, \mathbf{H}^*) + \iota_{S_2}(\mathbf{H}^*) \leq f(\mathbf{A}^*, \mathbf{Z}^*, \mathbf{H}) + \iota_{S_2}(\mathbf{H}), \forall \mathbf{H}$$

$$f(\mathbf{A}^*, \mathbf{Z}^*, \mathbf{H}^*) \leq f(\mathbf{A}, \mathbf{Z}^*, \mathbf{H}^*), \forall \mathbf{A}$$

$$f(\mathbf{A}^*, \mathbf{Z}^*, \mathbf{H}^*) + \iota_{S_1}(\mathbf{Z}^*) \leq f(\mathbf{A}^*, \mathbf{Z}, \mathbf{H}^*) + \iota_{S_1}(\mathbf{Z}), \forall \mathbf{Z}$$

which implies

$$0 \in \partial_{\mathbf{H}}(f(\mathbf{A}^*, \mathbf{Z}^*, \mathbf{H}^*) + \iota_{S_1}(\mathbf{Z}^*) + \iota_{S_2}(\mathbf{H}^*))$$

$$0 \in \partial_{\mathbf{A}}(f(\mathbf{A}^*, \mathbf{Z}^*, \mathbf{H}^*) + \iota_{S_1}(\mathbf{Z}^*) + \iota_{S_2}(\mathbf{H}^*))$$

$$0 \in \partial_{\mathbf{Z}}(f(\mathbf{A}^*, \mathbf{Z}^*, \mathbf{H}^*) + \iota_{S_1}(\mathbf{Z}^*) + \iota_{S_2}(\mathbf{H}^*))$$

Thus  $(\mathbf{A}^*, \mathbf{Z}^*, \mathbf{H}^*)$  is a stationary point of (13). ■

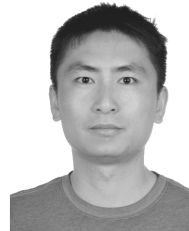
## REFERENCES

- [1] K. Wagstaff, C. Cardie, S. Rogers, S. Schrödl *et al.*, "Constrained k-means clustering with background knowledge," in *Proc. Int. Conf. Mach. Learn.*, Jun. 2001, pp. 577–584.
- [2] S. Anand, S. Mittal, O. Tuzel, and P. Meer, "Semi-supervised kernel mean shift clustering," *IEEE Trans. Pattern Anal. Mach. Intell.*, vol. 36, no. 6, pp. 1201–1215, Oct. 2013.
- [3] H. Zeng and Y.-m. Cheung, "Semi-supervised maximum margin clustering with pairwise constraints," *IEEE Trans. Knowl. Data Eng.*, vol. 24, no. 5, pp. 926–939, Mar. 2011.
- [4] S. Xiong, J. Azimi, and X. Z. Fern, "Active learning of constraints for semi-supervised clustering," *IEEE Trans. Knowl. Data Eng.*, vol. 26, no. 1, pp. 43–54, Jan. 2013.
- [5] B. Kulis, S. Basu, I. Dhillon, and R. Mooney, "Semi-supervised graph clustering: a kernel approach," *Mach. Learn.*, vol. 74, no. 1, pp. 1–22, Jan. 2009.
- [6] S. Basu, M. Bilenko, and R. J. Mooney, "A probabilistic framework for semi-supervised clustering," in *Proc. ACM SIGKDD Int. Conf. Knowl. Discov. Data Mining*, Aug. 2004, pp. 59–68.
- [7] L. Bai, J. Liang, and F. Cao, "Semi-supervised clustering with constraints of different types from multiple information sources," *IEEE Trans. Pattern Anal. Mach. Intell.*, vol. 43, no. 9, pp. 3247–3258, Mar. 2020.
- [8] R. Zass and A. Shashua, "A unifying approach to hard and probabilistic clustering," in *Proc. IEEE Int. Conf. Comput. Vis.*, vol. 1, Oct. 2005, pp. 294–301.
- [9] K. Thangavel and A. K. Mohideen, "Semi-supervised k-means clustering for outlier detection in mammogram classification," in *Proc. 2010 Trendz Inf. Sci. Comput.*, Dec. 2010, pp. 68–72.
- [10] R. Huang and W. Lam, "An active learning framework for semi-supervised document clustering with language modeling," *Data Knowl. Eng.*, vol. 68, no. 1, pp. 49–67, Jan. 2009.
- [11] Z. Yu, Z. Kuang, J. Liu, H. Chen, J. Zhang, J. You, H.-S. Wong, and G. Han, "Adaptive ensembling of semi-supervised clustering solutions," *IEEE Trans. Knowl. Data Eng.*, vol. 29, no. 8, pp. 1577–1590, Apr. 2017.
- [12] I. Ahn and C. Kim, "Face and hair region labeling using semi-supervised spectral clustering-based multiple segmentations," *IEEE Trans. Multimedia*, vol. 18, no. 7, pp. 1414–1421, Apr. 2016.
- [13] S. Saha, A. K. Alok, and A. Ekbal, "Brain image segmentation using semi-supervised clustering," *Expert Syst. Appl.*, vol. 52, pp. 50–63, Jun. 2016.
- [14] L. Yang, X. Cao, D. Jin, X. Wang, and D. Meng, "A unified semi-supervised community detection framework using latent space graph regularization," *IEEE Trans. Cybern.*, vol. 45, no. 11, pp. 2585–2598, Dec. 2014.
- [15] X. Li, Y. Wu, M. Ester, B. Kao, X. Wang, and Y. Zheng, "Semi-supervised clustering in attributed heterogeneous information networks," in *Proc. 26th Int. Conf. World Wide Web*, Apr. 2017, pp. 1621–1629.
- [16] A. Y. Ng, M. I. Jordan, and Y. Weiss, "On spectral clustering: Analysis and an algorithm," in *Proc. Adv. Neural Inf. Process. Syst.*, 2002, pp. 849–856.
- [17] Y. Jia, S. Kwong, and J. Hou, "Semi-supervised spectral clustering with structured sparsity regularization," *IEEE Signal Process. Lett.*, vol. 25, no. 3, pp. 403–407, Jan. 2018.
- [18] K. Kamvar, S. Sepandar, K. Klein, D. Dan, M. Manning, and C. Christopher, "Spectral learning," in *Proc. Int. Joint Conf. Artif. Intell.*, Apr. 2003, pp. 561–566.
- [19] F. Wang, C. Ding, and T. Li, "Integrated kl (k-means-laplacian) clustering: a new clustering approach by combining attribute data and pairwise relations," in *Proc. SIAM Int. Conf. Data Mining*, Apr. 2009, pp. 38–48.
- [20] Z. Lu and M. A. Carreira-Perpinan, "Constrained spectral clustering through affinity propagation," in *Proc. IEEE Conf. Comput. Vis. Pattern Recognit.*, Jun. 2008, pp. 1–8.

- [21] F. Nie, H. Zhang, R. Wang, and X. Li, "Semi-supervised clustering via pairwise constrained optimal graph," in *Proc. Int. Joint Conf. Artif. Intell.*, Jan. 2021, pp. 3160–3166.
- [22] Z. Li, J. Liu, and X. Tang, "Constrained clustering via spectral regularization," in *Proc. IEEE Conf. Comput. Vis. Pattern Recognit.*, Jun. 2009, pp. 421–428.
- [23] X. Wang and I. Davidson, "Flexible constrained spectral clustering," in *Proc. ACM SIGKDD Int. Conf. Knowl. Discov. Data Mining*, Jul. 2010, pp. 563–572.
- [24] X. Wang, B. Qian, and I. Davidson, "On constrained spectral clustering and its applications," *Data Mining Knowl. Discov.*, vol. 28, no. 1, pp. 1–30, Jan. 2014.
- [25] X. Fang, Y. Xu, X. Li, Z. Lai, and W. K. Wong, "Robust semi-supervised subspace clustering via non-negative low-rank representation," *IEEE Trans. Cybern.*, vol. 46, no. 8, pp. 1828–1838, Aug. 2015.
- [26] C.-G. Li, Z. Lin, H. Zhang, and J. Guo, "Learning semi-supervised representation towards a unified optimization framework for semi-supervised learning," in *Proc. IEEE Int. Conf. Comput. Vis.*, 2015, pp. 2767–2775.
- [27] W. Wang, C. Yang, H. Chen, and X. Feng, "Unified discriminative and coherent semi-supervised subspace clustering," *IEEE Trans. Image Process.*, vol. 27, no. 5, pp. 2461–2470, Feb. 2018.
- [28] M. Belkin and P. Niyogi, "Semi-supervised learning on riemannian manifolds," *Mach. Learn.*, vol. 56, no. 1, pp. 209–239, Jul. 2004.
- [29] X. Zhu, Z. Ghahramani, and J. D. Lafferty, "Semi-supervised learning using gaussian fields and harmonic functions," in *Proc. 20th Int. Conf. Mach. Learn.*, 2003, pp. 912–919.
- [30] L. K. Saul and S. T. Roweis, "Think globally, fit locally: unsupervised learning of low dimensional manifolds," *J. Mach. Learn. Res.*, vol. 4, no. 2, pp. 119–155, Jun. 2003.
- [31] F. Wang and C. Zhang, "Label propagation through linear neighborhoods," *IEEE Trans. Knowl. Data Eng.*, vol. 20, no. 1, pp. 55–67, Nov. 2007.
- [32] S. Yan and H. Wang, "Semi-supervised learning by sparse representation," in *Proc. SIAM Int. Conf. Data Mining*, Apr. 2009, pp. 788–797.
- [33] J. Chen and J. Yang, "Robust subspace segmentation via low-rank representation," *IEEE Trans. Cybern.*, vol. 44, no. 8, pp. 1432–1445, Nov. 2013.
- [34] C. Lu, J. Feng, Z. Lin, T. Mei, and S. Yan, "Subspace clustering by block diagonal representation," *IEEE Trans. Pattern Anal. Mach. Intell.*, vol. 41, no. 2, pp. 487–501, Jan. 2018.
- [35] E. Elhamifar and R. Vidal, "Sparse subspace clustering: Algorithm, theory, and applications," *IEEE Trans. Pattern Anal. Mach. Intell.*, vol. 35, no. 11, pp. 2765–2781, Mar. 2013.
- [36] J. Zhang, C.-G. Li, C. You, X. Qi, H. Zhang, J. Guo, and Z. Lin, "Self-supervised convolutional subspace clustering network," in *Proc. IEEE Conf. Comput. Vis. Pattern Recognit.*, 2019, pp. 5473–5482.
- [37] Y. Yang, J. Feng, N. Jojic, J. Yang, and T. S. Huang, " $\ell^0$ -sparse subspace clustering," in *Proc. Eur. Conf. Comput. Vis.*, Oct. 2016, pp. 731–747.
- [38] L.-H. Zhang, L.-Z. Liao, and M. K. Ng, "Fast algorithms for the generalized foley-sammon discriminant analysis," *SIAM J. Matrix Anal. Appl.*, vol. 31, no. 4, pp. 1584–1605, 2010.
- [39] Y. Jia, F. Nie, and C. Zhang, "Trace ratio problem revisited," *IEEE Trans. Neural Netw. Learn. Syst.*, vol. 20, no. 4, pp. 729–735, Mar. 2009.
- [40] T. T. Ngo, M. Bellalij, and Y. Saad, "The trace ratio optimization problem," *SIAM Rev.*, vol. 54, no. 3, pp. 545–569, 2012.
- [41] L. Zhuang, H. Gao, Z. Lin, Y. Ma, X. Zhang, and N. Yu, "Non-negative low rank and sparse graph for semi-supervised learning," in *Proc. IEEE Conf. Comput. Vis. Pattern Recognit.*, Jun. 2012, pp. 2328–2335.
- [42] D. Cai, X. He, and J. Han, "Spectral regression for efficient regularized subspace learning," in *Proc. IEEE Int. Conf. Comput. Vis.*, Oct. 2007, pp. 1–8.
- [43] X. He, S. Yan, Y. Hu, P. Niyogi, and H.-J. Zhang, "Face recognition using laplacianfaces," *IEEE Trans. Pattern Anal. Mach. Intell.*, vol. 27, no. 3, pp. 328–340, Jan. 2005.
- [44] D. Cai, X. He, and J. Han, "Speed up kernel discriminant analysis," *VLDB J.*, vol. 20, no. 1, pp. 21–33, Feb. 2011.
- [45] D. Cai, X. He, J. Han, and H.-J. Zhang, "Orthogonal laplacianfaces for face recognition," *IEEE Trans. Image Process.*, vol. 15, no. 11, pp. 3608–3614, Oct. 2006.
- [46] Z. Li, J. Tang, and X. He, "Robust structured nonnegative matrix factorization for image representation," *IEEE Trans. Neural Netw. Learn. Syst.*, vol. 29, no. 5, pp. 1947–1960, May 2018.
- [47] P. Sen, G. Namata, M. Bilgic, L. Getoor, B. Galligher, and T. Eliassi-Rad, "Collective classification in network data," *AI Mag.*, vol. 29, no. 3, pp. 93–93, Sep. 2008.
- [48] Y. Feng, H. You, Z. Zhang, R. Ji, and Y. Gao, "Hypergraph neural networks," in *Proc. AAAI Conf. Artif. Intell.*, Jul. 2019, pp. 3558–3565.
- [49] D. Zhou, J. Huang, and B. Schölkopf, "Learning with hypergraphs: Clustering, classification, and embedding," in *Proc. Adv. Neural Inf. Process. Syst.*, 2006, pp. 1601–1608.
- [50] J. Mairal, "Optimization with first-order surrogate functions," in *Proc. Int. Conf. Mach. Learn.*, May 2013, pp. 783–791.



**Huaming Ling** received the B.S. degree from Sun Yat-Sen University. He is currently pursuing the Ph.D. degree with the Department of Mathematics, Tsinghua University. His main research interests include pattern recognition, computer vision and machine learning.



**Chenglong Bao** is an assistant professor in Yau Mathematical Sciences Center, Tsinghua University and Yanqi Lake Beijing Institute of Mathematical Sciences and Applications. He received his Ph.D. from the department of mathematics, National University of Singapore in 2014. His main research interests include mathematical image processing, large scale optimization and its applications.



**Xin Liang** is an assistant professor in Yau Mathematical Sciences Center, Tsinghua University and Yanqi Lake Beijing Institute of Mathematical Sciences and Applications. He received his Ph.D. from the School of Mathematical Sciences, Peking University in 2014. His main research interests include numerical linear algebra, matrix analysis, and their applications.



**Zuoqiang Shi** is a professor in Yau Mathematical Sciences Center, Tsinghua University and Yanqi Lake Beijing Institute of Mathematical Sciences and Applications. He received his Ph.D. from Zhou Pei-Yuan Center for Applied Mathematics, Tsinghua University in 2008. His main research interests include numerical methods of partial differential equations and their applications, mathematical image processing.